Effects of H₂O on liquidus phase relations in the haplogranite system at 2 and 5 kbar

François Holtz*

Institut für Mineralogie, Universität Hannover, Welfengarten 1, D-3000 Hannover 1, Germany
and Centre de Recherches sur la Synthèse et la Chimie des Minéraux, CNRS, 1A, rue de la Férollerie, 45071 Orléans Cedex 02, France

Michel Pichavant*

Centre de Recherche Pétrographiques et Géochimiques, CNRS, B.P. 20, 54501 Vandoeuvre les Nancy, France
and Centre de Recherches sur la Synthèse et la Chimie des Minéraux, CNRS, 1A, rue de la Férollerie, 45071 Orléans Cedex 02, France

Pierre Barbey

Université de Nancy I, Laboratoire de Pétrologie, B.P. 239, 54506 Vandoeuvre les Nancy Cedex, France
and Centre de Recherche Pétrographiques et Géochimiques, CNRS, B.P. 20, 54501 Vandoeuvre les Nancy, France

Wilhelm Johannes

Institut für Mineralogie, Universität Hannover, Welfengarten 1, D-3000 Hannover 1, Germany

Abstract

Liquidus phase relations have been experimentally determined in the system Qz-Or-Ab at 2 and 5 kbar under both H₂O-saturated and H₂O-undersaturated conditions. Crystallization experiments were conducted with dry synthetic glasses as starting materials. Reversals used partially crystallized glasses. H₂O-undersaturated conditions were obtained by using H₂O-CO₂ fluid mixtures. Six liquidus surfaces, corresponding to an initial fluid phase composition [$X_{H_2O}^{In}$ = H₂O/(H₂O + CO₂) initial] of 1, 0.7, and 0.5 at 2 kbar and 1, 0.85, and 0.7 at 5 kbar, were studied. Small ratios of fluid to silicate were used, and the equilibruim fluid phase composition [H₂O/(H₂O + CO₂)] differs from $X_{H_2O}^{In}$. For both pressures, H₂O solubilities decrease with decreasing $X_{H_2O}^{In}$. H₂O activities (a_{H_2O}), calculated for compositions close to the thermal minimum of the corresponding liquidus surface are 1, 0.5, and 0.25 at 2 kbar and 1, 0.6, and 0.4 at 5 kbar. General agreement is noted between crystallization and reversal experiments, both in terms of liquidus temperatures and phase compositions.

Our data for H₂O-saturated conditions are in good agreement with Tuttle and Bowen (1958) at 2 kbar. At 5 kbar, our quartz-feldspar field boundary is richer in normative quartz by 2–6 wt%, compared with Luth et al. (1964). At both pressures, decreasing the H₂O content of the melt causes a rise in liquidus temperatures for all studied compositions and a progressive shift of minimum and eutectic compositions toward the Qz-Or join at approximately content normative quartz content. The rise in liquidus temperatures with decreasing H₂O contrast of the melt is more marked for Ab- than for Or-rich compositions. The observed changes in phase relations contrast with the results of calculations using the model of Burnham and Nekvasil (1986) for hydrous aluminosilicate melts. Our results suggest a differential reactivity of Ab- and Or-forming units in the melt with H₂O, consistent with higher H₂O solubilities in Ab-rich than in Or-rich melts. Application of the results to natural magmatic systems allows the effect of pressure and of the H₂O content of the melt on residual granitic liquid compositions to be specified individually.

Introduction

This paper presents new experimental data on liquidus phase relations in both the H₂O-saturated and H₂O-undersaturated parts of the haplogranite system SiO₂-KAlSi₃O₈-NaAlSi₃O₈ (Qz-Or-Ab) at 2 and 5 kbar. It complements the recent study of Ebadi and Johannes (1991) on solidus phase relations under H₂O-undersaturated

conditions. The main objective in this paper is to show experimentally the effect of isobaric changes of H₂O content of the melt on liquidus phase relations. The investigation is particularly focused on (1) the effect of H₂O on the primary quartz and feldspar liquidus fields, (2) the composition of ternary minimum or eutectic points, and (3) the liquidus temperatures.

Although there has been a considerable amount of work done on solidus and liquidus phase relations in the H₂O-saturated haplogranite system (e.g., Goranson, 1938; Tuttle and Bowen, 1958; Luth et al., 1964; Boettcher and

* Present address: Centre de Recherches sur la Synthèse et Chimie des Minéraux, CRSCM-CNRS 1A, rue de la Férollerie, 45071 Orléans Cedex, France.

Wyllie, 1969; James and Hamilton, 1969; Merrill et al., 1970; Steiner et al., 1975; Huang and Wyllie, 1975, 1986; Winkler, 1979; Johannes, 1980, 1984), until recently little direct experimental information has been available for H_2O-undersaturated conditions in this fundamental system (Wyllie and Tuttle, 1959; Luth, 1969; Huang and Wyllie, 1975; Steiner et al., 1975; Whitney, 1975; Keppler, 1989; Ebadi and Johannes, 1991). In the system Qz-Or-Ab-B_2O_3, at 1 kbar, Pichavant and Ramboz (1985) and Pichavant (1987) first demonstrated a shift in the minimum liquidus compositions toward the Qz-Or binary join at approximately constant normative Qz with isobaric reduction of the H_2O content of the melt. This change in phase relations is in apparent conflict with calculations performed for the system Qz-Or-Ab (Nekvasil and Burnham, 1987), which predict a shift of the minimum liquidus composition away from the Qz apex toward the alkali feldspar join under the same conditions. The experimental determination of the individual effect of the H_2O content of the melt on phase relations is of critical importance given (1) the now-general agreement that most granitic magmas evolve under H_2O-undersaturated conditions (e.g., Burnham, 1967; Luth, 1969; Maaloe and Wyllie, 1975), (2) recent progress in estimating the H_2O contents and volatile distribution in magma chambers (reviewed by Clemens, 1984; see also Pichavant et al., 1988; Anderson et al., 1989) and (3) the current debate about H_2O solubility mechanisms in aluminosilicate melts (e.g., Burnham, 1981; Stolper, 1982; McMillan and Holloway, 1987; Silver and Stolper, 1989; Kohn et al., 1989; Silver et al., 1990).

EXPERIMENTAL METHODS

The purpose of this study is to determine experimentally the effects of isobaric change in the melt H_2O content, i.e., a_{H_2O} (H_2O activity), on liquidus phase relations in the system SiO_2-$KAlSi_3O_8$-$NaAlSi_3O_8$. The effect of a_{H_2O} on solidus temperatures was investigated recently by Keppler (1989) and Ebadi and Johannes (1991) and is not considered here.

For both pressures investigated (2 and 5 kbar), three liquidus surfaces were determined: one for H_2O-saturated and two for H_2O-undersaturated conditions. The 2- and 5-kbar H_2O-saturated liquidus experiments duplicate those of Tuttle and Bowen (1958) and Luth et al. (1964), respectively. They were carried out as a test of the reliability of our experimental methods as well as those of the earlier studies. Furthermore, they provide a direct, unambiguous comparison between the H_2O-saturated and H_2O-undersaturated liquidus surfaces.

Starting materials

Dry synthetic glasses with various compositions in the Qz-Or-Ab, Qz-Ab, and Qz-Or systems were made from gels prepared using TEOS (tetraethylorthosilicate), aluminum nitrate, and nitrates or carbonates of potassium and sodium. Some glasses were also synthesized from mixtures of previously prepared gels. After drying, the gels were melted at temperatures between 1250 and 1400 °C in welded Pt capsules for approximately 4 h. For each starting glass, two cycles of melting and grinding were performed to improve its chemical homogeneity. Two bubble-free glasses (obtained from D. B. Dingwell and R. P. Taylor) were also used for the determination of H_2O contents by the Karl Fischer titration method. All glasses were analyzed by electron microprobe (compositions given in Table 1). They do not deviate significantly from the Qz-Or-Ab plane. Some are weakly peraluminous and others weakly peralkaline. However, all ternary glass compositions used in the experiments have more than 99 wt% normative Qz + Or + Ab.

H_2O and H_2O-CO_2 mixtures were used for H_2O-saturated and H_2O-undersaturated experiments, respectively. Thus, a fluid phase was always present in our experiments. Doubly distilled deionized H_2O was used as a source of H_2O. The $Ag_2C_2O_4$ used as a source of CO_2 was synthesized from silver nitrate and oxalic acid, and the CO_2 yield calibrated (97%). Care was taken to keep constant the proportion of fluid components (H_2O + CO_2) in the sample for each set of experiments (Wyllie and Tuttle, 1960, 1961; Boettcher, 1984). For the H_2O-saturated experiments [$X_{H_2O}^{In}$ = $H_2O/(H_2O + CO_2)$ initial = 1], all samples contained 10 wt% H_2O for the 2-kbar experiments and 15 wt% H_2O for the 5-kbar experiments (90 and 85 wt% dry silicate glass, respectively). For the H_2O-undersaturated experiments ($X_{H_2O}^{In} < 1$), a constant proportion of 10 wt% (H_2O + CO_2) was chosen, irrespective of pressure. Consequently, fluid to silicate ratios were small throughout this study. We chose to have small ratios to avoid large changes in the starting glass composition caused by incongruent dissolution in the fluid phase. The initial fluid compositions ($X_{H_2O}^{In}$) were 1, 0.7, and 0.5 at 2 kbar and 1, 0.85, and 0.7 at 5 kbar. Because of our small fluid to silicate ratios and our initially dry starting glasses, the equilibrium fluid phase composition differs from the initial fluid phase composition (Fig. 1). The samples (typically 20 mg of glass crushed to a grain size less than 50 μm, plus the required amount of the fluid components) were loaded in Au capsules (25–15 mm long; id 2.5 mm; thickness 0.20–0.25 mm), which were closed by welding.

Apparatus and experimental procedure

This study was carried out simultaneously in two experimental laboratories: the 2-kbar and part of the 5-kbar H_2O-saturated experiments were performed in the CRPG (Nancy, France); all the H_2O-undersaturated and the remaining part of the 5-kbar H_2O-saturated experiments were performed in the Institute of Mineralogy of the University of Hanover (Germany).

In Nancy, all experiments were made in René 41 cold-seal pressure vessels (rapid quench for 2 kbar and horizontal Tuttle type for 5 kbar) pressurized with Ar. Each vessel-furnace pair was carefully calibrated for temperature under pressure, using internal dual-sheathed chromel-alumel thermocouples calibrated against melting of

TABLE 1. Composition and CIPW norm of the starting glasses

Glass no.	442	433	424	$3_{75}42_{25}$	3_542_5	3_533_5	3_524_5	3_33_29	$3_43_33_3$	$3_32_54_2$ (TB)	$3_{25}33_{75}$
n	(6)	(3)	(13)	(calc)	(14)	(9)	(8)	(7)	(5)	(5)	(calc)
SiO$_2$	80.68	80.28	80.22	78.93	77.56	79.23	79.43	77.78	78.11	79.45	78.11
Al$_2$O$_3$	11.32	11.36	11.35	12.01	12.69	12.61	12.51	12.80	12.61	12.63	12.85
K$_2$O	6.43	5.08	3.37	6.68	6.98	4.80	3.18	6.28	5.51	4.40	4.87
Na$_2$O	2.23	3.57	4.64	2.63	3.15	3.98	5.18	3.50	3.99	4.64	4.33
Total	100.66	100.29	99.58	100.25	100.38	100.62	100.30	100.36	100.22	101.12	100.16
Qz	42.9	40.0	40.5	37.9	33.0	37.5	37.0	33.3	33.7	35.3	34.2
Or	37.7	29.9	19.9	39.4	40.6	28.2	18.7	37.0	32.5	25.7	28.7
Ab	18.7	30.1	39.4	22.2	26.2	33.5	43.8	29.5	33.7	38.8	36.6
Co	0.7	—	—	0.5	—	0.8	0.5	0.2	0.1	0.2	0.5
KS	—	—	0.1	—	0.1	—	—	—	—	—	—
NaS	—	—	0.1	—	0.1	—	—	—	—	—	—

Glass no.	3_12_47 (LJT)	352	343	334	325	2_543_5	2_534_5	2_525_5	4_65_40	4_55_60	4_25_80
n	(5)	(6)	(5)	(6)	(11)	(6)	(11)	(4)	(4)	(6)	(4)
SiO$_2$	76.91	75.81	76.85	77.07	78.02	75.08	75.53	74.78	80.79	80.04	79.25
Al$_2$O$_3$	13.49	13.19	13.33	13.34	13.36	14.08	14.67	14.60	10.48	10.52	10.80
K$_2$O	3.58	8.27	6.72	4.94	3.31	6.82	5.03	3.42	9.06	9.25	9.50
Na$_2$O	5.57	2.37	3.47	4.74	5.66	4.15	5.15	6.67	0.03	0.00	0.00
Total	99.55	99.64	100.37	100.09	100.35	100.13	100.38	99.47	100.36	99.81	99.55
Qz	31.0	30.5	30.8	30.6	32.3	25.2	26.2	23.2	46.0	44.7	43.1
Or	21.3	49.1	39.6	29.2	19.5	39.8	29.6	20.2	53.4	54.8	56.4
Ab	47.3	20.1	29.3	40.0	47.8	34.8	43.4	56.5	0.0	0.0	0.0
Co	0.4	0.3	0.3	0.2	0.4	—	0.8	—	0.6	0.5	0.5
KS	—	—	—	—	—	0.1	—	—	—	—	—
NaS	—	—	—	—	—	0.1	—	0.1	—	—	—

Glass no.	460	3_56_50	370	4_05_7	3_606_4	$3_{35}06_{65}$	$3,06_9$	307	$3_62_53_9$*	$3_73_52_8$*
n	(6)	(6)	(8)	(11)	(7)	(9)	(4)	(10)	(10)	(10)
SiO$_2$	79.25	77.47	76.14	80.95	80.55	79.64	78.09	78.02	79.10	78.82
Al$_2$O$_3$	11.05	11.86	13.14	12.66	12.73	13.11	14.16	13.73	12.07	11.83
K$_2$O	10.16	10.58	11.08	0.00	0.00	0.00	0.02	0.05	4.23	5.89
Na$_2$O	0.00	0.01	0.00	6.68	6.93	7.29	8.08	8.20	4.60	3.46
Total	100.46	99.92	100.36	100.29	100.21	100.04	100.35	100.00	100.00	100.00
Qz	40.2	37.0	33.6	42.0	40.2	37.2	31.0	30.3	36.4	36.9
Or	59.7	62.6	65.3	0.0	0.0	0.0	0.0	0.0	25.0	34.8
Ab	0.0	0.0	0.0	56.3	58.5	61.7	68.1	69.5	38.5	28.0
Co	0.1	0.4	1.1	1.7	1.3	1.1	0.9	0.2	—	—
KS	—	—	—	—	—	—	—	—	—	—
NaS	—	—	—	—	—	—	—	—	0.1	0.3

Note: no = glass labeled after the normative Qz/Or/Ab proportions (composition 3_542_5 contains approximately 35% Qz, 40% Or, 25% Ab); n = average of n microprobe analyses; TB = 2-kbar minimum composition (Tuttle and Bowen, 1958); LJT = 5-kbar minimum composition (Luth et al., 1964); calc = composition calculated (glass prepared by mixing two gels of known compositions); Co = normative corundum; KS = K$_2$SiO$_3$; NaS = Na$_2$SiO$_3$.

* Bubble-free starting glasses, analyses from Holtz et al. (1992a).

NaCl, Zn, and Sn (Pichavant, 1987). The overall maximum error on the recorded temperatures is less than ±10 °C. Pressure was measured with a 7-kbar Heise gauge (error ±20 bars) and checked periodically. In Hanover, horizontal cold-seal pressure vessels made of ATS 290 were employed. Temperatures were measured by external Ni-CrNi thermocouples calibrated against certified thermocouples and are known to be accurate to within 2% (Puziewicz and Johannes, 1988). Pressure (H$_2$O pressure medium) was measured with a strain gauge manometer (accuracy ±50 bars, precision 20 bars). For the series of experiments that was shared between the two laboratories (5 kbar, $X_{H_2O}^{In} = 1$), no evidence was found from the results for any significant interlaboratory inconsistency in either temperature or pressure calibration and measurement. We also found no evidence for an influence of f_{H_2} on the results (the experiments performed in Hanover had a higher f_{H_2} than those conducted in Nancy).

Several capsules were placed side by side in the same vessel. Heating time ranged between 30 and 180 min, starting from an initially applied pressure of 50–90% of the desired pressure, depending on the equipment. Duration varied between 90 and about 1200 h for the low temperature reversal experiments. Quenching was performed under pressure. A decrease of temperature down to 300 °C was reached in 5 s to 4 min, depending on the equipment. After a check for leaks, the capsules were opened and the experimental products examined by petrographic techniques. X-ray diffraction was used for identification and for the analysis of feldspar (Johannes, 1979; Orville, 1963); electron microprobes were used to analyze experimental glasses and alkali feldspars.

For a given Qz-Or-Ab composition, the liquidus temperature is the temperature of the equilibrium liquid (L) + crystals (Ctx) + fluid (V) = L + V. In this study the liquidus temperature was determined from both sides of
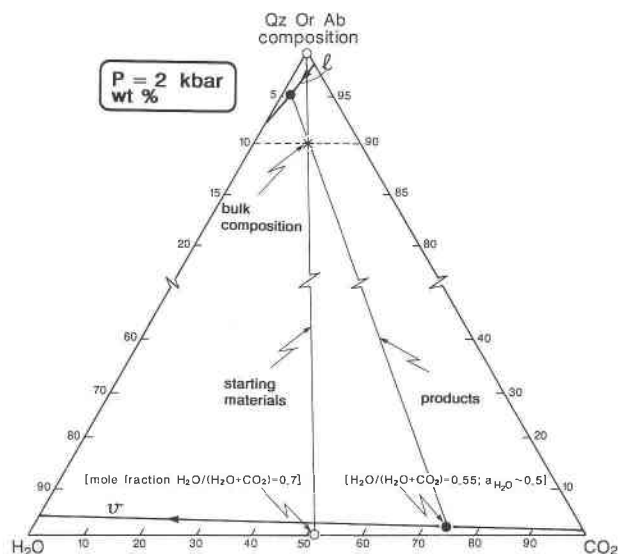
Fig. 1. Polythermal isobaric (2 kbar) representation of the phase relations in the system Qz-Ab-Or-H_2O-CO_2 showing the evolution of the fluid phase composition in our liquidus experiments with H_2O-CO_2 fluid mixtures (see also Wyllie and Tuttle, 1960, 1961; Boettcher, 1984). Open symbols = starting materials (dry Qz-Ab-Or glass and H_2O-CO_2 fluid mixture); filled symbols = equilibrium composition of experimental products (hydrous melt and CO_2-enriched fluid mixture). Note that the final fluid phase composition and melt H_2O content (hence a_{H_2O}) is dependent on the fluid to silicate ratio in the charge. In the figure, scale is distorted for clarity, as the solubility of CO_2 in the melt is considered to be negligible (see text).

the equilibrium, i.e., by crystallization and dissolution experiments. The presence of crystals and crystal growth (idiomorphic crystals) was taken as evidence for partial crystallization (L + Ctx + V field), whereas the absence of crystals combined with crystal resorption (rounded morphologies) indicated supraliquidus conditions (L + V field). Crystallization experiments approached the liqui-

dus temperature from the high-temperature side. They were conducted from crystal-free glasses at intervals of approximately 20 °C down to the appearance of crystalline phases in the experimental products. Reversal experiments consisted of two stages. In the first stage, the temperature was one known to produce partial crystallization, according to the forward experiments. In the second stage, the temperature was raised isobarically to the final value. Therefore, the reversal experiments approached the liquidus temperature from the low-temperature side by using partially crystallized samples. Usual temperature intervals between reversals were 10 °C. Reversal experiments were systematically carried out at 2 kbar, $X_{H_2O}^{In} = 1$ and 0.7 and at 5 kbar, $X_{H_2O}^{In} = 1$ and 0.85. Given the agreement between the two types of experiments under these conditions, it was not considered necessary to perform systematic reversal experiments for the two highest temperature series (2 kbar, $X_{H_2O}^{In} = 0.5$; 5 kbar, $X_{H_2O}^{In} = 0.7$).

Analytical techniques

Two Camebax electron microprobes (University of Nancy, University of Hanover) were used to analyze glasses and feldspars for their major elements. These were operated under the following conditions: acceleration voltage, 15 kV; sample current 6–8 nA (Nancy) and 18 nA (Hanover); counting time of 6 s on peak for all elements (Nancy), 2 s for Na and K and 5 s for Si and Al (Hanover). Silicate standards and ZAF correction procedures were utilized. For the analysis of alkalis in glasses, we used a defocused beam of 10–20 μm on both instruments. In addition, secondary standard hydrous granitic glasses, analyzed for Na_2O and K_2O by wet chemical techniques, were systematically probed, together with the experimental samples, in order to determine correction factors for the alkalis (Pichavant, 1987). There was generally no need for corrections of the electron microprobe data for dry and H_2O-undersaturated glasses, whereas for H_2O-saturated glasses, Na_2O had to be cor-

TABLE 2. Comparison of compositions of dry and hydrous supraliquidus glasses analyzed by electron microprobe

Glass no.	424* st	424** st	424**	424*	433*	3₅42₅**
n	4	9	5	4	3	5
T (°C)	—	—	825 845	740	740	705
P (kbar)	—	—	2	2	2	5
$X_{H_2O}^{In}$	—	—	0.7	1	1	1
SiO_2	80.03(0.54)	80.30(0.23)	77.59(0.30)	73.00(0.97)	74.41(0.26)	69.98(0.45)
Al_2O_3	11.17(0.25)	11.43(0.29)	11.23(0.23)	10.60(0.11)	10.48(0.14)	11.15(0.13)
K_2O	3.32(0.13)	3.39(0.13)	3.25(0.17)	3.03(0.12)	4.75(0.06)	6.02(0.21)
Na_2O	4.62(0.05)	4.65(0.22)	4.52(0.13)	4.30(0.21)	3.22(0.08)	2.79(0.09)
Total	99.14(0.29)	99.77(0.45)	96.59(0.26)	90.93(0.91)	92.86(0.10)	89.94(0.35)
Qz	40.6	40.4	40.3	40.0	40.4	34.2
Or	19.6	20.1	19.9	19.7	30.2	39.5
Ab	39.4	39.4	39.5	40.0	29.3	26.2
Co	—	0.1	0.3	0.3	—	0.1
KS	0.2	—	—	—	—	—
NaS	0.2	—	—	—	—	—

Note: st = starting glass; n = average value of n analyses; numbers in parentheses = standard deviation (1σ).
* Analyzed with the Nancy electron microprobe.
** Analyzed with the Hanover electron microprobe.

TABLE 3. Experimental results for 2 kbar, $X^{In}_{H_2O} = 1.0$

Glass no.	T (°C)		Duration (h)	Results	Feld. comp. (mol% Or)	Liquidus T
433	740		213	L		720–740
	720		290	L + Qz		(730)
424	740		131	L		720–740
	720		290	L + Qz		(730)
3_542_5	750		240	L		720–750
	720		528	L + Sa	Or_{84}	(750)
	720	750	288 168	L + (Sa) diss.		
3_533_5	700		480	L + (Qz)		700–710
	680		648	L + Qz + Sa	Or_{73}	(710)
	680 (1–2 kbar)	700	480 528	L + Qz + (Sa)		
	680	710	552 408	L		
3_524_5	700		480	L + (Qz)		700–710
	680		648	L + Qz + Sa	Or_{10}	(710)
	680 (1–2 kbar)	700	480 528	L + Qz + Sa		
	680	710	552 408	L		
334	726		213	L		715–726
	700		290	L + Sa	Or_{67}	(720)
	700	715	480 360	L + Sa diss.		
	700	730	456 240	L		
325	727		213	L		700–715
	700		290	L + Sa	Or_8	(710)
	700	715	480 360	L		
$3_32_54_2$	685		576	L + (Qz + Sa)	Or_{47}	≥685

Note: Experiments performed in Nancy. The liquidus temperatures given in parentheses are those reported in the phase diagram (Fig. 2). Experiments with two temperatures and durations are two-stage reversal experiments. In two reversal experiments both pressure and temperature were varied (680 °C, 1 kbar to 700 °C, 2 kbar). L = liquid; Qz = quartz; Sa = alkali feldspar solid solution; diss. = crystals dissolving; phases in parentheses denote very low amounts.

rected upward by variable but significant factors (Nancy, 1.03–1.05; Hanover, 1.10–1.12), because of the migration of Na.

The quality of our microprobe analyses of glasses was carefully checked (Table 2). (1) The reproducibility of the data was tested by periodically analyzing several of the starting glasses. (2) Seven starting glasses were analyzed in duplicate with the two electron microprobes. Slightly higher normative corundum values were obtained with the Hanover microprobe than with the Nancy microprobe (maximum difference 0.5%, Table 2). However, all glasses were found to have Qz-Or-Ab compositions identical within 2% normative, and six of the seven glasses were within 1% normative. For these glasses, the data from both instruments have been averaged in Table 1. (3) The normative composition of hydrous supraliquidus glasses has been compared with that of the dry starting glasses. Excellent agreement is noted between the two types of glasses, irrespective of their Na₂O/K₂O ratios and H₂O contents (Tables 1 and 2), and this demonstrates our ability in electron microprobe analysis of hydrous glasses. (4) For subliquidus experiments, colinearity between experimental products and starting materials provides a further check of electron microprobe data (see below).

The H₂O contents of supraliquidus experimental glasses were determined by the Karl Fischer titration method (Westrich, 1987; Holtz et al., 1992a). The Karl Fischer method was carried out on the bubble-free glasses (uncertainty: ±0.15 wt% H₂O). The experimental and analytical procedures follow those of Holtz et al. (1992a). Other supraliquidus glasses were analyzed for their H₂O

and CO₂ contents by micromanometry in the stable isotope laboratory of CRPG (C. France-Lanord, analyst; uncertainty: ±0.2 wt% H₂O).

Results

Products

Experimental results at 2 kbar ($X^{In}_{H_2O} = 1$, 0.7, and 0.5) are given in Tables 3–5 and at 5 kbar ($X^{In}_{H_2O} = 1$, 0.85, and 0.7) in Tables 6–8. Silicate glass with numerous, mostly spherical, fluid inclusions is the major solid experimental product. Quartz and feldspar are the only crystalline phases found; their size is usually smaller in H₂O-undersaturated than in H₂O-saturated experiments (maximum feldspar size 25 and 40 μm, respectively; quartz size always less than 5 μm). Analytical data for melts coexisting with crystals (feldspar, or feldspar + quartz) are in Table 9, and feldspar compositions are given in Table 10.

H₂O, CO₂, and a_{H_2O}

Melts. The H₂O contents of supraliquidus glasses (Table 11) were determined at 2 and 5 kbar and for $X^{In}_{H_2O} = 1$, 0.7, 0.5 and 1, 0.85, 0.7, respectively. The compositions of the glasses were chosen to be close to the minima and eutectics found in this study (glass nos. $3_62_53_9$, $3_73_52_8$, 334, see Table 1). At both pressures, the H₂O contents of the melt progressively decrease with decreasing $X^{In}_{H_2O}$ (Table 11). At 2 kbar, for $X^{In}_{H_2O} = 0.7$ and T between 825 and 880 °C, H₂O contents obtained by the Karl Fischer titration and manometric measurement are in good

TABLE 4. Experimental results for 2 kbar, $X_{H_2O}^{in} = 0.7$

Glass no.	T (°C)	Duration (h)	Results	Feld. comp. (mol% Or)	Liquidus T
442	850	188	L		830–840
	830	141	L + Qz		(840)
	820 830	96 140	L + Qz		
	820 840	121 126	L		
433	830	141	L		825–830
	810	217	L + Qz		(825)
	795 825	142 125	L + Qz		
	810 840	240 139	L		
424	850	122	L		840–845
	840	116	L + (Qz)		(840)
	810	116	L + Qz		
	815 835	121 126	L + Qz		
	815 845	142 125	L		
3_542_5	815	366	L		810–815
	810	159	L + Sa		(815)
	790 810	240 139	L + Sa	Or_{81}	
	790 820	243 145	L		
3_533_5	805	167	L + (Qz)		805–810
	780	121	L + Qz		(810)
	780 790	96 144	L + Qz		
	780 800	121 126	L + (Qz)		
	780 810	118 120	L		
3_524_5	840	116	L		810–825
	810	116	L + Sa + Qz	Or_{10}	(820)
	790 810	96 144	L + (Qz)		
	800 825	96 144	L		
352	855	108	L + Sa	Or_{87}	>855
	835	304	L + Sa	Or_{87}	
343	835	304	L		820–830
	820	113	L + (Sa)		(825)
	780	151	L + Sa + Qz	Or_{74}	
	790 810	240 139	L + Sa	Or_{74}	
	800 820	143 148	L + (Sa)		
	800 830	142 125	L		
334	835	108	L		810–825
	780	122	L + Sa + Qz	Or_{37-40}	(810)
	770 790	96 144	L + Sa		
	790 810	96 144	L + (Sa)		
	795 825	142 125	L		
325	835	108	L		820–825
	820	113	L + (Sa)		(825)
	795 815	140 118	L + Sa		
	800 820	140 118	L + (Sa)		
	800 825	96 144	L		
2_543_5	845	190	L		840–845
	830	143	L + Sa		(840)
	815 835	140 118	L + Sa		
	815 840	140 118	L + Sa		
	815 845	118 143	L		
2_534_5	830	165	L		820–830
	795 815	96 144	L + Sa		(825)
	800 820	140 118	L + (Sa)		
	800 830	118 145	L		

Note: Experiments performed in Hanover. The liquidus temperatures given in parentheses are those reported in the phase diagram (Fig. 3). Experiments with two temperatures and durations are two-stage reversal experiments. Same abbreviations as in Table 3.

agreement (see Table 11). For H₂O-saturated conditions, our data at 2 kbar (average: 5.9 wt% H₂O) are also in agreement with those of Tuttle and Bowen (1958), i.e., 5.86 and 6.66 wt% H₂O. Luth (1976) gives a saturation limit of 6.5 wt% H₂O at 2 kbar. At 5 kbar and under H₂O-saturated conditions, a H₂O content of 9.85 is found in this study (Table 11), lower than the 11 wt% given by Luth (1976).

The micromanometric measurements performed for glass no. 334 on samples analyzed for their H₂O contents (Table 11) did not reveal the presence of any CO₂, implying that CO₂ solubility in these glasses is less than the detection limit (0.3 wt% CO₂ under our analytical conditions). CO₂ can thus be considered to be nearly insoluble in the aluminosilicate melts studied here, in agreement with conclusions from other studies (e.g., Boettcher et al., 1987; Fogel and Rutherford, 1990).

Fluid phase. The composition of the fluid phase in equilibrium with melt at P and T was determined by the study of fluid inclusions trapped in glass. Glasses formed at 2 kbar contained a single type of fluid inclusion, which is interpreted to represent trapped fluids in equilibrium with melt at P and T (i.e., final entrapment probably takes place during quench at the glass transition). On the other

hand, the 5-kbar glasses commonly showed evidence for reequilibration revealed by the presence of an additional population of inclusions with sizes in the micrometer range, spherical shape, and uniform distribution throughout the sample. Two-phase (liquid H_2O, supercritical CO_2) and three-phase (liquid H_2O, liquid CO_2, and vapor CO_2) inclusions were encountered. Some were studied by microthermometric methods (Pichavant and Ramboz, 1985; Pichavant, 1987) and Raman microprobe (Instituut voor Aardwetenschappen, Amsterdam, and CREGU, Vandoeuvre les Nancy) in order to determine their bulk composition (Ramboz et al., 1985). For a given sample, phase assemblages and volumetric proportions as well as analytical results were found to be nearly identical, thus indicating a compositionally homogeneous fluid phase. Raman analysis showed no evidence of H_2 or carbonic species other than CO_2 that could be indicative of partial reduction of the H_2O-CO_2 fluid mixture. However, the presence of N_2 (from the air trapped in the capsule) was demonstrated from the CO_2 freezing-point depression and the vibrational mode at 2335 cm⁻¹ in the Raman spectrum (compare Pichavant, 1987). Therefore, the fluid phases in this study are dominantly composed of H_2O, CO_2, and N_2 (between 2.5 and 7 mol% N_2 in 2-kbar experiments, depending on the size of the capsule and $X_{H_2O}^{In}$; less than 2 mol% in 5-kbar experiments because these capsules were crimped prior to welding). Fluid inclusions trapped in glass no. 334 at 2 kbar, 850 °C, and $X_{H_2O}^{In} = 0.7$ contain 40 mol% H_2O, 54 mol% CO_2, and 6 mol% N_2 (starting fluid phase: 68 mol% H_2O, 27 mol% CO_2, 5 mol% N_2), confirming that initial and equilibrium fluid compositions differ in their $H_2O/(H_2O + CO_2)$ ratio (Fig. 1). The lack of silicate daughter crystals in the analyzed fluid inclusions indicates small silicate solute concentrations in the fluid phase.

Evaluation of a_{H_2O}. The activity of H_2O was calculated by two methods, but only for ternary compositions close to the minima and eutectics. (1) Using the model of Burnham (1979) and our experimentally determined H_2O contents of the melt, a_{H_2O} of 0.97, 0.50, and 0.26 were calculated at 2 kbar for $X_{H_2O}^{In}$ of 1, 0.7, and 0.5, respectively (Table 11). At 5 kbar, a_{H_2O} of 0.98, 0.57, and 0.39 were calculated for $X_{H_2O}^{In}$ of 1, 0.85, and 0.7, respectively (Table 11). Note that these H_2O activities are computed from data obtained at experimental temperatures higher than the liquidus temperatures (Table 11). However, because of the small temperature dependence of the H_2O solubility (Hamilton and Oxtoby, 1986; Holtz et al., 1992a), this will only affect calculated a_{H_2O} by 0.02–0.01. (2) The H_2O activity was also calculated from the fluid phase composition, using the modified Redlich-Kwong equation (Kerrick and Jacobs, 1981). In this calculation, N_2 was treated as an inert diluent. The composition of the fluid phase was that determined in glass no. 334 at 850 °C, 2 kbar, and $X_{H_2O}^{In} = 0.7$ (40 mol% H_2O, 54 mol% CO_2, 6 mol% N_2). The a_{H_2O} was found to be 0.49, a value identical to that calculated from the H_2O content of the melt in the same experiment (see Table 11).

TABLE 5. Experimental results for 2 kbar, $X_{H_2O}^{In} = 0.5$

Glass no.	T (°C)	Duration (h)	Results	Feld. comp. (mol% Or)	Liquidus T (°C)
424	875	117	L + Qz		>875
3₅42₅	850	95	L + ((Sa))	Or₇₆	>850
	835	169	L + Sa	Or₇₃	(855)
3₅33₅	865	196	L		855–865
	855	95	L + (Qz)		(855)
3₅24₅	865	169	L		845–865
	845	196	L + (Qz) + ((Sa))	Or₁₄	(860)
3,3,2₉	860	314	L		840–860
	840	196	L + (Sa)		(845)
	830	169	L + Sa	Or₆₉	
3,3,3₃	860	314	L		840–860
	840	196	L + (Sa)	Or₅₉	(840)
	835	169	L + Qz + Sa	Or₅₆	
352	870	144	L + Sa		>870
343	865	196	L		855–865
	855	149	L + (Sa)		(855)
	835	119	L + Sa	Or₇₁	
334	855	149	L		835–855
	835	119	L + Sa	Or₃₁	(850)
325	870	117	L + Sa		>870
2₅43₅	875	96	L + Sa		>875
2₅34₅	875	96	L		855–875
	855	314	L + (Sa)		(860)

Note: Experiments performed in Hanover. The liquidus temperatures given in parentheses are those reported in the phase diagram (Fig. 4). Experiments with two temperatures and durations are two-stage reversal experiments. Same abbreviations as in Table 3. Phases indicated in double parentheses denote that only traces have been detected in the experimental products.

An independent test of our a_{H_2O} values was performed by comparing the four H_2O-undersaturated minimum liquidus temperatures (this study) with the solidus temperatures for a given a_{H_2O} (Ebadi and Johannes, 1991). When reported on their P-T-a_{H_2O} diagram (Fig. 10 in Ebadi and Johannes, 1991), our four H_2O-undersaturated minimum liquidus temperatures indicate a_{H_2O} of 0.5 and 0.3 for 2 kbar and 0.6 and 0.45 for 5 kbar. These a_{H_2O} values are in good agreement with those obtained from the H_2O contents of our supraliquidus melts and fluid phase compositions (see Table 11). We emphasize that the a_{H_2O} values given in this study for the four H_2O-undersaturated sections apply only to compositions close to their corresponding minima. Partial crystallization is not expected to affect significantly the calculated a_{H_2O}, given the range of crystal fractions in our liquidus experiments [generally below 5 wt%; with exceptions as high as 14 wt% in some H_2O-undersaturated experiments (see glass no. 343, Table 5 and Fig. 4) and as high as 18 wt% in some H_2O-saturated experiments (see glass no. 2₅25₅, Table 6 and Fig. 5; the proportions of the crystals have been determined from the lever rule)].

Liquidus temperatures

Liquidus temperature brackets are mostly within 20 °C (the temperature uncertainty on each boundary is ±10 °C), except for a few compositions having wider brackets. These temperature brackets are established by considering, for each composition, results from both crystallization and reversal experiments, thus implying an overall

HOLTZ ET AL.: H$_2$O IN THE HAPLOGRANITE SYSTEM

TABLE 6. Experimental results for 5 kbar, $X^{in}_{H_2O} = 1.0$

Glass no.	T (°C)	Duration (h)	Results	Feld. comp. (mol% Or)	Liquidus T
3_542_5	705	525	L		700–705
	685	525	L + Or	Or$_{91}$	(705)
	675 685	720 477	L + Or	Or$_{90}$	
	675 705	505 570	L + ((Or))		
$3_43_72_9$	675	796	L + Or	Or$_{87}$	695–705
	675 695	720 477	L + (Or)	Or$_{89}$	(695)
	675 705	505 570	L		
$3_43_33_3$	680	796	L		665–680
	650 665	366 505	L + Qz + Or		(675)
	680 700	720 477	L		
$3_{25}33_{75}$	690	525	L		680–690
	680	796	L + (Qz) + ((Or))		(685)
	655	796	L + Qz + Or	Or$_{79}$	
$3_12_24_7$*	660	532	L		650–660
	650	648	L + (Qz)		(650)
	640	504	L + Qz + Ab	Or$_{9}$	
343	710	525	L		690–700
	690	525	L + Or	Or$_{89}$	(705)
	680 700	720 477	L + Or	Or$_{89}$	
	680 710	505 570	L		
334	675	525	L		660–670
	660	796	L + *Or* + Qz	Or$_{80}$	(665)
	655 670	366 505	L		
325	675	796	L		660–670
	660	796	L + Qz		(665)
	655	796	L + Qz + ((Or))		
	655 670	366 505	L		
2_534_5*	680	332	L		660–680
	660	532	L + Or	Or$_{71}$	(675)
	660 680	532 789	L + (Or) diss.		
2_525_5*	680	332	L		660–680
	660	532	L + Ab	Or$_{12}$	(670)
	660 680	532 789	L		

Note: The liquidus temperatures given in parentheses are those reported in the phase diagram (Fig. 5). Experiments with two temperatures and durations are two-stage reversal experiments. Same abbreviations as in Table 3 and Or = K-rich alkali feldspar; Ab = Na-rich alkali feldspar. Phases indicated in double parentheses denote that only traces have been detected in the experimental products. Italicized phases denote that significant amounts are present in the experimental products.
* Experiments performed in Nancy, all others in Hanover.

excellent agreement between both types of experiments. A few problems between the crystallization and reversal experiments were noted for some compositions in the feldspar primary field. Feldspar crystals persist in some reversals at higher temperatures than indicated by the crystallization experiments (nos. 3_524_5, 3_533_5, Table 3; 2_534_5, Table 6; 3_542_5, Table 7), suggesting either slow dissolution kinetics of alkali feldspar in the melt (in the reversal experiments) or nucleation problems (in the crystallization experiment). The opposite, feldspar crystals growing at temperatures higher than indicated by the reversals, has also been encountered (composition no. 3_524_5, Table 4), although in only one experiment. However, these problems have a minor effect on liquidus temperature, and they are clearly exceptions, given the large number of experiments carried out during this study (about 400). It must be pointed out that only three liquidus temperature brackets are available for the 5-kbar, $X^{in}_{H_2O} = 0.7$ section (Table 8) because experimental temperatures were close to the upper limit of our equipment. Note that the "liquidus temperatures" given in Tables 3–8 are preferred values established from experimental data and observations (the amount of crystals present in the subliquidus experiments being an indication of the temperature interval between liquidus and the experimental temperature).

Melt compositions

The compositions of glasses coexisting with either alkali feldspar or alkali feldspar plus quartz (Table 9) are either slightly peralkaline or peraluminous (corundum normative). Most glasses have small amounts (≤ 0.6 wt%) of normative corundum, except four glasses with values higher than 1 wt%, of which none has more than 1.7 wt% normative corundum. For subliquidus melts, colinearity between starting and experimental products is generally satisfied on the ternary phase diagrams (Figs. 2–7). In cases where experiments in which quartz, alkali feldspar, and melt are coexisting, all three-phase triangles enclose the starting composition. Note that the tie lines and three-phase triangles are mainly drawn from the crystallization experiments.

Alkali feldspars

The compositions of the alkali feldspars obtained by electron microprobe analysis and X-ray techniques are identical within error. Structural formulae, calculated from electron microprobe data on the basis of 16 O atoms, are of good quality for alkali feldspars, except for a few that

TABLE 7. Experimental results for 5 kbar, $X_{H_2O}^{In} = 0.85$

Glass no.	T (°C)	Duration (h)	Results	Feld. comp. (mol% Or)	Liquidus T
424	810	149	L + Qz		>810
$3_{75}42_{25}$	770	92	L + Qz		>770
3_542_5	780	123	L		780–790
	760	168	L + Sa	Or₈₆	(785)
	740 770	118 168	L + Sa	Or₈₆	
	750 780	136 149	L + (Sa)		
3_524_5	800	120	L		795–800
	780	123	L + Qz		(795)
	760 785	120 96	L + Qz		
	765 795	184 125	L + (Qz)		
$3_43_33_3$	770	149	L		765–770
	750	168	L + Qz + (Sa)		(765)
	725 745	120 96	L + Qz + Sa		
	725 755	184 125	L + Qz + (Sa)	Or₇₆	
	725 765	360 166	L + (Qz)		
	725 775	123 165	L		
$3_{25}33_{75}$	770	92	L + ((Qz))		770–780
					(775)
352	820	170	L		805–820
	800	120	L + Sa	Or₉₁	(815)
343	800	143	L		780–790
	785	121	L + ((Sa))		(785)
	755 780	118 168	L + (Sa)	Or₈₃	
	765 790	120 96	L		
334	760	239	L		745–760
	745	122	L + Sa	Or₆₈	(750)
	730 740	120 96	L + Sa + (Qz)		
	730 760	184 125	L		
325	765	239	L		760–770
	750	168	L + Qz		(765)
	740	118	L + *Qz* + Sa	Or₈	
	730 750	120 96	L + Qz		
	730 760	184 125	L + (Qz)		
2_543_5	810	149	L		790–800
	790	120	L + Sa		(800)
	765 790	120 96	L + Sa		
	770 800	184 125	L		
2_534_5	800	143	L		770–775
	775	121	L + (Sa)	Or₄₆₋₄₈	(775)
	740	122	L + Sa		
	760 775	118 168	L		

Note: Experiments performed in Hanover. The liquidus temperatures given in parentheses are those reported in the phase diagram (Fig. 6). Experiments with two temperatures and durations are two-stage reversal experiments. Same abbreviations as in Table 3. Phases indicated in double parentheses denote that only traces have been detected in the experimental products. Italicized phases denote that significant amounts are present in the experimental products.

show anomalously high Si (Table 10). These anomalous values probably result from analytical overlap on the surrounding glass. In general, for a given sample, the alkali feldspar composition is homogeneous within ±1 mol% Or, except for some intermediate compositions (Or_{35}–Or_{60}) that show intrasample variations of 5 mol%. Although, in this case, the two extreme compositional bounds are given [compositions 334 at 2 kbar, $X_{H_2O}^{In} = 0.7$, and 2_534_5 at 5 kbar, $X_{H_2O}^{In} = 0.85$; see Table 10], only one composition (arbitrarily chosen to be the highest in Ab content) is plotted on the phase diagrams. For a given bulk composition, alkali feldspars analyzed in crystallization and reversal experiments have compositions always within 2 mol% Or (Tables 4, 6, 7, 10).

Ternary phase diagrams

The results are projected isobarically into the anhydrous system Qz-Or-Ab (Figs. 2–7), as was done in earlier studies (e.g., Tuttle and Bowen, 1958; Luth et al., 1964) in order to facilitate comparison.

Liquidus phases, liquidus temperatures, and compositions of alkali feldspars and coexisting melts were used to define the primary liquidus phase fields, the position of the cotectic or quartz-feldspar boundary curve, isotherms on the liquidus surfaces, and tie lines and three-phase triangles. In addition, the minimum liquidus temperature point (the lowest temperature point, either of minimum type or of eutectic type, along a cotectic line or the quartz-feldspar boundary curve) was determined graphically from tie lines and three-phase triangles. Some phase diagrams (Figs. 2–5) were constructed by including data (liquidus temperatures and compositions of eutectic points) for the Qz-Or and the Qz-Ab binary systems (detailed in Pichavant et al., 1992).

For all 2-kbar experiments, the investigated temperatures lie above the critical temperature of the alkali feldspar solvus (660 °C at 1 kbar; Brown and Parsons, 1980). Therefore, phase diagrams (Figs. 2–4) are divided into two fields (feldspar solid solution and quartz primary fields) separated by a cotectic line with a minimum (e.g.,

TABLE 8. Experimental results for 5 kbar, $X^{In}_{H_2O} = 0.7$

Glass no.	T (°C)	Dura-tion (h)	Results	Feld. comp. (mol% Or)	Liquidus T
$3_{75}42_{25}$	805	92	L + *Qz* + Sa		>805
3_542_5	815	106	L		805–815
	805		L + Sa	Or_{83}	(815)
3_524_5	815	106	L + Qz		>815
$3_43_72_9$	815	142	L		800–810
	805	170	L + (Ctx)		(805)
	800	120	L + Sa + Qz	Or_{78}	
$3_{25}33_{75}$	805	92	L + Qz + (Sa)		>805
343	820	136	L + ((Sa))	Or_{80}	≥820
334	820	136	L		805–815
	805	116	L + ((Sa))		(805)
	800	121	L + Sa + (Qz)	Or_{50}	
325	820	117	L + (Sa)	Or_{10}	>820
2_543_5	820	126	L + Sa		>820
2_534_5	820	126	L + Sa	Or_{37}	>820

Note: Experiments performed in Hanover. The liquidus temperatures given in parentheses are those reported in the phase diagram (Fig. 7). Experiments with two temperatures and durations are two-stage reversal experiments. Same abbreviations as in Table 3. Ctx indicates presence of quartz or feldspar phases. Phases indicated in double parentheses denote that only traces have been detected in the experimental products. Italicized phases denote that significant amounts are present in the experimental products.

Luth, 1976). Similar phase relations were also obtained at 5 kbar for the H₂O-undersaturated conditions studied. In contrast, at 5 kbar and for H₂O-saturated conditions, liquidus temperatures are low enough to intersect the alkali feldspar solvus (720 °C; Brown and Parsons, 1980) and three primary phase fields (Fig. 5) must be present
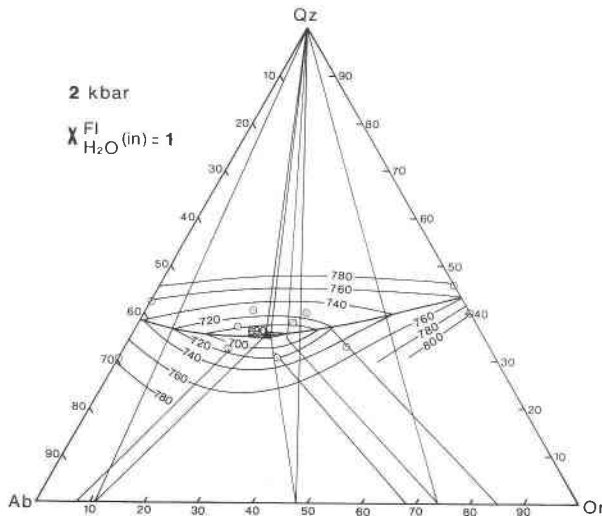

Fig. 2. Liquidus phase relations in the system Qz-Ab-Or-H₂O at 2 kbar for a fluid phase with an initial mole fraction H₂O/(H₂O + CO₂) = $X^{In}_{H_2O} = 1$ (H₂O-saturated conditions). Experimental results are given in Table 3. Isotherms are labeled in degrees Celsius. Dots represent the investigated compositions (given in Table 1); the position of the minimum liquidus point of the system is given by the solid triangle. The composition of melts and feldspars used for the construction of conjugation lines and three-phase triangles are given in Tables 9 and 10, respectively.
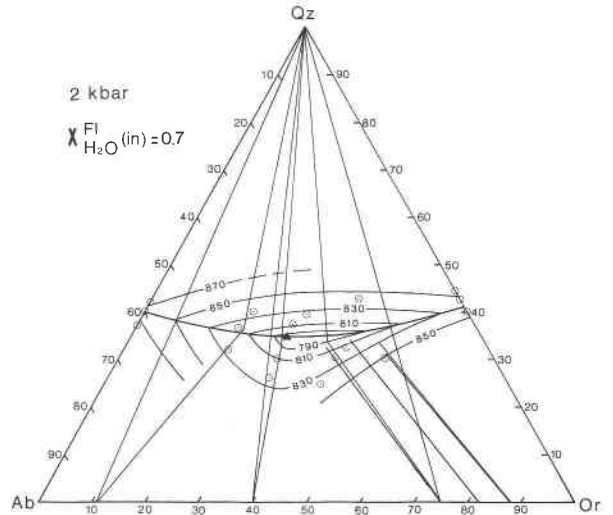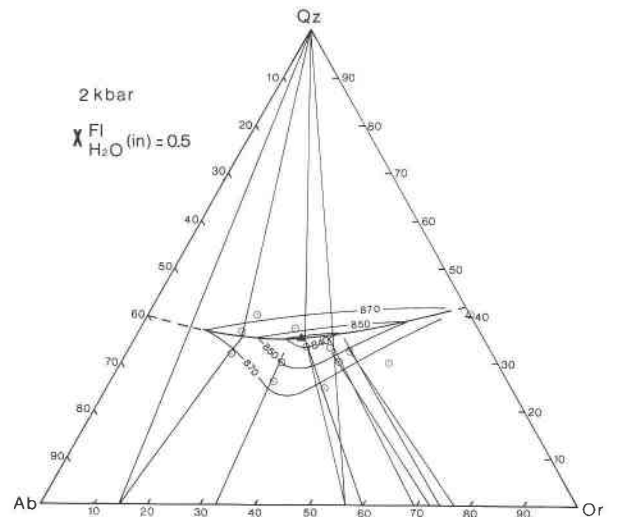

Fig. 3. Liquidus phase relations in the system Qz-Ab-Or-H₂O-CO₂ at 2 kbar for a fluid phase with $X^{In}_{H_2O} = 0.7$. Experimental results are given in Table 4. Symbols and sources of data as in Figure 2.

on the liquidus (e.g., Luth, 1976). Although our experiments do not bring direct information about the existence of two feldspar primary fields, a boundary curve, passing between composition nos. 2_534_5 and 2_525_5 (Table 6), has been constructed on Figure 5. In this isobaric section (5 kbar, $X^{In}_{H_2O} = 1$), feldspar compositions show a gap between Or_{12} and Or_{71} (Fig. 5) corresponding to the intersected solvus.

For the two pressures investigated, there is a comparable evolution of the ternary phase relations with decreasing $X^{In}_{H_2O}$ and a_{H_2O}:

1. Liquidus temperatures progressively increase for all

Fig. 4. Liquidus phase relations in the system Qz-Ab-Or-H₂O-CO₂ at 2 kbar for a fluid phase with $X^{In}_{H_2O} = 0.5$. Experimental results are given in Table 5. Symbols and sources of data as in Figure 2.

TABLE 9. Composition and CIPW norm of glasses coexisting with crystals

Glass no.	3_542_5	3_533_5	3_524_5	$3_25_42_2$	334	325	3_542_5	3_524_5	352	352	343	343	334	3_542_5	3_542_5
n	3	3	3	4	3	3	4	4	8	8	8	4	6	6	9
T (°C)	720	680	680	685	700	700	790 810	810	835	855	780	790 810	780	850	835
P (kbar)	2	2	2	2	2	2	2	2	2	2	2	2	2	2	2
$X_{H_2O}^{in}$	1	1	1	1	1	1	0.7	0.7	0.7	0.7	0.7	0.7	0.7	0.5	0.5
SiO₂	73.16	72.35	72.46	73.51	71.17	70.30	75.57	76.27	74.48	73.52	74.89	74.43	74.59	74.35	75.18
Al₂O₃	11.26	11.74	11.45	11.72	11.99	12.21	12.15	11.88	12.38	12.57	12.47	12.23	12.78	12.21	12.43
K₂O	2.97	4.57	3.86	3.99	4.38	3.01	6.71	3.23	7.65	7.97	5.96	6.08	4.71	6.54	6.31
Na₂O	5.68	3.97	4.30	4.28	4.34	5.15	2.82	4.54	2.24	2.15	3.32	3.32	4.33	2.93	2.89
Total	93.07	92.63	92.07	93.50	91.88	90.67	97.25	95.92	96.77	96.21	96.64	96.06	96.31	96.03	96.81
Qz	36.7	34.3	35.5	35.7	31.7	31.8	34.4	37.0	33.4	31.7	33.9	33.1	32.5	33.6	35.3
Or	36.1	29.2	24.8	25.2	28.2	19.6	40.8	20.1	46.6	49.0	36.3	37.5	28.9	40.2	38.5
Ab	27.0	36.3	39.5	38.7	40.0	48.1	24.5	42.5	19.6	18.9	29.2	29.2	38.0	25.8	25.3
Co	0.2	0.2	0.2	0.4	0.1	0.5	0.3	0.4	0.4	0.4	0.6	0.2	0.6	0.4	0.9
KS	—	—	—	—	—	—	—	—	—	—	—	—	—	—	—
NaS	—	—	—	—	—	—	—	—	—	—	—	—	—	—	—

Glass no.	3_524_5	$3_43_72_9$	$3_43_33_3$	$3_43_33_3$	343	334	3_542_5	3_542_5	$3_43_72_9$	$3_43_72_9$	$3_{25}33_{75}$	3_12_47	343	334	2_534_5
n	6	7	4	6	8	5	3	5	3	3	3	7	5	3	4
T (°C)	845	830	840	835	835	835	685	675 685	675	675 695	655	640	690	660	660
P (kbar)	2	2	2	2	2	2	5	5	5	5	5	5	5	5	5
$X_{H_2O}^{in}$	0.5	0.5	0.5	0.5	0.5	0.5	1	1	1	1	1	1	1	1	1
SiO₂	76.24	76.42	76.76	76.36	75.62	75.10	69.12	70.72	69.15	70.62	68.79	68.97	68.22	70.14	69.42
Al₂O₃	12.16	12.28	12.36	12.42	12.66	12.88	10.92	11.19	11.25	11.31	12.25	12.19	11.36	11.80	12.98
K₂O	5.17	5.82	5.74	5.23	6.19	4.70	5.94	5.88	5.39	5.77	3.88	3.32	5.90	4.31	3.84
Na₂O	3.15	3.29	3.78	3.77	3.42	4.39	2.66	2.62	3.29	2.93	4.17	5.01	3.12	4.42	4.74
Total	96.72	97.81	98.64	97.78	97.89	97.07	88.64	90.41	89.08	90.63	89.09	89.49	88.60	90.67	90.98
Qz	35.2	35.7	33.6	35.1	32.7	32.6	34.9	36.5	33.1	34.8	33.4	30.4	31.8	31.5	29.9
Or	19.3	35.2	32.0	31.6	37.3	28.6	39.6	38.5	35.8	37.7	25.8	21.9	39.4	28.2	25.0
Ab	45.2	28.5	34.4	32.7	29.6	38.2	25.4	24.5	31.1	27.3	39.6	47.3	28.8	40.3	44.0
Co	0.3	0.6	—	0.6	0.4	0.6	0.1	0.5	—	0.2	1.2	0.4	—	—	1.1
KS	—	—	—	—	—	—	—	—	—	—	—	—	—	—	—
NaS	—	—	—	—	—	—	—	—	—	—	—	—	—	—	—

Glass no.	2_525_5	3_542_5	3_542_5	$3_43_33_3$	352	343	334	325	2_534_5	3_542_5	$3_43_72_9$	343	334	325	2_534_5
n	4	5	4	5	5	5	4	6	9	5	7	7	7	7	7
T (°C)	660	760	740 770	725 755	800	755 780	745	740	775	805	800	820	800	820	820
P (kbar)	5	5	5	5	5	5	5	5	5	5	5	5	5	5	5
$X_{H_2O}^{in}$	1	0.85	0.85	0.85	0.85	0.85	0.85	0.85	0.85	0.7	0.7	0.7	0.7	0.7	0.7
SiO₂	69.76	71.91	71.80	71.57	71.57	71.42	71.86	71.82	68.64	73.63	73.54	71.78	71.75	72.28	72.07
Al₂O₃	12.55	11.56	11.36	11.56	11.64	12.07	11.99	12.29	13.34	11.69	11.61	12.32	12.40	12.48	13.36
K₂O	3.15	6.21	6.10	5.13	7.63	6.25	4.71	3.81	4.56	4.46	6.38	5.92	4.60	3.07	4.63
Na₂O	5.32	2.52	2.56	3.50	2.16	3.17	4.18	4.64	4.46	2.85	3.23	3.09	4.35	5.27	4.08
Total	90.78	92.20	91.82	91.76	93.00	92.91	92.94	92.56	91.00	94.55	94.30	93.55	93.10	93.10	94.14
Qz	29.5	36.2	36.6	34.6	31.9	31.2	31.8	32.7	27.8	34.5	34.0	31.5	31.0	32.1	32.6
Or	20.5	39.8	39.3	33.1	48.3	39.8	30.1	24.4	29.6	39.9	37.0	40.2	29.2	19.5	29.1
Ab	49.6	23.1	23.6	32.2	19.6	28.9	38.1	42.4	41.4	25.4	28.9	27.9	39.5	47.9	36.6
Co	0.4	0.7	0.5	0.3	—	0.1	—	0.5	1.2	0.2	0.1	0.4	—	0.5	1.7
KS	—	—	—	—	0.1	—	—	—	—	—	—	—	—	—	—
NaS	—	—	—	—	0.1	—	—	—	—	—	—	—	—	—	—

Note: Same as in Table 1.

compositions, the increase being more pronounced for Qz-Ab than for Qz-Or-rich compositions (Fig. 8).

2. No significant compositional shift in the position of the cotectic curve (2 kbar) and the quartz-feldspar field boundary (5 kbar) is observed.

3. Eutectic or minimum liquidus temperature points move progressively toward increasing Or contents at approximately constant normative Qz (Fig. 9); compositions and temperatures of the minima and eutectic are summarized in Table 12. Uncertainties in the position of these minimum liquidus temperature points can be estimated by summing the analytical uncertainties (electron microprobe analyses, see standard deviations in Table 2)

and errors due to the construction of the phase diagrams. These latter uncertainties are difficult to evaluate. Moreover, they depend on the isobaric section considered (compare Figs. 2 and 7). At worst, the composition of minimum liquidus temperature points is given with uncertainties of ±2.5 wt% normative Qz and ±2 wt% normative Ab and Or (Table 11).

DISCUSSION

The attainment of equilibrium

Reaction mechanisms in our experiments include three main processes: (1) incorporation of H₂O from the fluid

TABLE 10. Composition of alkali feldspars coexisting with glass and glass + quartz

Glass no.	3_542_5	3_533_5	3_524_5	$3_22_54_2$	334	325	3_524_5	352	352	343	343	334
T (°C)	720	680	680	685	700	700	810	835	855	780	790 810	780
P (kbar)	2	2	2	2	2	2	2	2	2	2	2	2
$X_{H_2O}^{In}$	1	1	1	1	1	1	0.7	0.7	0.7	0.7	0.7	0.7
SiO₂	67.55	67.58	68.28	70.25	66.97	67.87	69.57	65.36	65.89	67.00	67.48	67.92
Al₂O₃	18.28	18.71	18.82	18.22	18.57	18.71	18.77	18.20	17.60	18.22	18.03	18.76
K₂O	13.86	12.35	1.79	7.69	11.38	1.44	1.71	14.14	14.48	12.42	12.62	6.23
Na₂O	1.73	3.08	10.13	5.77	3.75	10.68	10.29	1.45	1.39	2.86	2.92	6.98
Total	101.42	101.72	99.02	101.93	100.67	98.70	100.34	99.15	99.36	100.50	101.05	99.90
Si	6.07	6.04	6.04	6.14	6.03	6.03	6.06	6.03	6.08	6.06	6.07	6.04
Al	1.94	1.97	1.96	1.88	1.97	1.96	1.93	1.98	1.91	1.94	1.91	1.97
K	1.59	1.41	0.20	0.86	1.31	0.16	0.19	1.66	1.71	1.44	1.45	0.71
Na	0.30	0.53	1.74	0.98	0.66	1.84	1.74	0.26	0.25	0.50	0.51	1.21
KAlSi₃O₈ (mol%)	84	73	10	47	67	8	10	87	87	74	74	37

Glass no.	334	3_542_5	3_542_5	3_524_5	$3_43_72_9$	$3_43_33_3$	$3_43_33_3$	343	334	3_542_5	3_542_5	$3_43_72_9$
T (°C)	780	850	835	845	830	840	835	835	835	685	675 685	675
P (kbar)	2	2	2	2	2	2	2	2	2	5	5	5
$X_{H_2O}^{In}$	0.7	0.5	0.5	0.5	0.5	0.5	0.5	0.5	0.5	1	1	1
SiO₂	68.29	66.17	66.55	73.02	66.87	67.14	66.78	66.82	67.43	65.26	65.28	63.73
Al₂O₃	18.55	18.31	18.05	17.44	18.24	18.67	18.45	18.68	18.30	17.79	17.82	17.54
K₂O	6.81	12.89	11.94	1.92	11.41	10.29	9.44	11.87	5.40	14.91	15.44	15.31
Na₂O	6.76	2.62	2.92	7.90	3.45	4.70	4.88	3.14	7.73	0.96	1.17	1.46
Total	100.41	99.99	99.46	100.28	99.97	100.80	99.55	100.51	98.86	98.92	99.71	98.04
Si	6.06	6.03	6.06	6.29	6.06	6.02	6.04	6.03	6.06	6.05	6.04	6.01
Al	1.94	1.97	1.94	1.77	1.95	1.98	1.97	1.99	1.94	1.95	1.94	1.95
K	0.77	1.50	1.39	0.21	1.31	1.18	1.09	1.37	0.62	1.76	1.82	1.84
Na	1.16	0.46	0.52	1.32	0.61	0.82	0.86	0.55	1.35	0.17	0.21	0.27
KAlSi₃O₈ (mol%)	40	76	73	14	69	59	56	71	31	91	90	87

Glass no.	$3_43_72_9$	$3_{25}33_{75}$	3_12_47	343	334	2_534_5	2_525_5	3_542_5	3_542_5	$3_43_33_3$	352	343
T (°C)	675 695	655	640	690	660	660	660	760	740 770	725 755	800	755 780
P (kbar)	5	5	5	5	5	5	5	5	5	5	5	5
$X_{H_2O}^{In}$	1	1	1	1	1	1	1	0.85	0.85	0.85	0.85	0.85
SiO₂	66.01	64.96	67.45	64.39	64.18	66.83	61.03	64.63	65.42	65.41	66.05	65.45
Al₂O₃	17.84	18.18	19.03	18.02	18.07	18.52	19.33	18.43	18.34	18.54	18.25	18.57
K₂O	15.05	12.87	1.81	14.86	13.88	12.16	2.21	14.66	14.60	13.10	15.79	14.14
Na₂O	1.19	2.29	11.19	1.19	2.34	3.32	10.18	1.57	1.59	2.64	1.03	1.83
Total	100.09	98.30	99.48	98.46	98.47	100.83	100.75	99.29	99.95	99.69	101.12	99.99
Si	6.06	6.02	5.98	6.01	5.99	6.02	6.02	5.99	6.01	6.00	6.04	6.00
Al	1.93	1.99	1.98	1.98	1.99	1.96	1.98	2.01	1.99	2.00	1.96	2.00
K	1.76	1.52	0.20	1.77	1.66	1.40	0.24	1.73	1.71	1.53	1.84	1.65
Na	0.21	0.41	1.92	0.22	0.42	0.58	1.72	0.28	0.28	0.47	0.18	0.33
KAlSi₃O₈ (mol%)	89	79	9	89	80	71	12	86	86	76	91	83

Glass no.	334	325	2_534_5		3_542_5	$3_43_72_9$	343	334	325	2_534_5
T (°C)	745	740	775		805	800	820	800	820	820
P (kbar)	5	5	5		5	5	5	5	5	5
$X_{H_2O}^{In}$	0.85	0.85	0.85		0.7	0.7	0.7	0.7	0.7	0.7
SiO₂	66.05	69.60	66.81	67.83	66.26	66.37	67.25	66.61	71.39	67.46
Al₂O₃	18.40	19.37	19.02	18.86	17.90	18.17	18.75	18.73	19.17	18.49
K₂O	11.63	1.42	8.10	8.33	14.11	13.35	13.52	8.55	1.49	6.44
Na₂O	3.61	10.29	6.19	5.91	1.96	2.48	2.26	5.57	8.82	7.21
Total	99.69	100.68	100.12	100.93	100.23	100.37	101.78	99.46	100.87	99.60
Si	6.02	6.04	5.99	6.03	6.06	6.04	6.03	6.01	6.13	6.04
Al	1.98	1.98	2.01	1.98	1.93	1.95	1.98	1.99	1.94	1.95
K	1.35	0.16	0.93	0.94	1.64	1.55	1.55	0.99	0.16	0.74
Na	0.64	1.74	1.08	1.02	0.35	0.44	0.39	0.98	1.47	1.25
KAlSi₃O₈ (mol%)	68	8	46	48	83	78	80	50	10	37

Note: Structural formulae calculated on the basis of 16 O atoms.

TABLE 11. H₂O contents of supraliquidus glasses

P (kbar)	$X^{in}_{H_2O}$	Glass no.	T (°C)	H₂O content (wt%)	a_{H_2O}*
2	1	3₆2₅3₉	800	5.94**	0.98
2	1	3₇3₅2₈	800	5.87**	0.97
2	0.7	3₆2₅3₉	880	3.46	0.52
2	0.7	3₇3₅2₈	880	3.19	0.47
2	0.7	334	825	3.72†	0.56
2	0.7	334	835	3.52†	0.52
2	0.7	334	850	3.39†	0.49
2	0.5	3₆2₅3₉	880	2.19	0.27
2	0.5	3₇3₅2₈	880	2.09	0.25
5	1	3₆2₅3₉	800	9.90	0.99
5	1	3₇3₅2₈	800	9.80	0.98
5	0.85	3₆2₅3₉	880	5.62	0.59
5	0.85	3₇3₅2₈	880	5.23	0.55
5	0.7	3₆2₅3₉	880	4.04	0.40
5	0.7	3₇3₅2₈	880	3.97	0.39

* Calculated from Burnham (1979).
** From Holtz et al. (1992a).
† H₂O analyzed by micromanometry (C. France-Lanord, CRPG). Karl Fischer titration used for all other analyses (experimental and analytical methods given in Holtz et al., 1992a).

Fig. 6. Liquidus phase relations in the system Qz-Ab-Or-H₂O-CO₂ at 5 kbar for a fluid phase with a $X^{in}_{H_2O} = 0.85$. Experimental results are given in Table 7. Symbols and sources of data as in Figure 2.

phase into the initially dry glass to produce a homogeneous hydrous melt, (2) nucleation and growth of crystals from that melt, and (3) dissolution of crystals (specific to reversal experiments). Discussing the attainment of equilibrium implies an evaluation of the kinetics of these three processes.

1. With an average grain size of 50 μm for the starting ground glass, times of a maximum of a few tens of minutes are sufficient for H₂O to diffuse throughout, if the experimental temperature is attained instantaneously (35 min at 750 °C, 17 min at 850 °C, diffusivities of H₂O at 2 kbar of H₂O pressure taken from Shaw, 1974; 8 min at 850 °C, diffusivities of H₂O at 5 kbar taken from Lapham et al., 1984). This suggests that the production of a homogeneous hydrous melt is rapid under our experimental conditions. Note that this remains true for the H₂O-undersaturated experiments because of the use of H₂O-CO₂ mixtures to control a_{H_2O}. An indication of a homogeneous distribution of H₂O in our hydrous melts is furnished by the microprobe data. For a given experimental glass, summation deficiencies do not show significant varia-

Fig. 5. Liquidus phase relations in the system Qz-Ab-Or-H₂O at 5 kbar for a fluid phase with a $X^{in}_{H_2O} = 1$ (H₂O-saturated conditions). Experimental results are given in Table 6. Symbols and sources of data as in Figure 2. In contrast to Figures 2–4, the feldspar solvus on the Ab-Or sideline is intersected, and three primary fields appear on the liquidus: albite solid solution, orthoclase solid solution, and quartz.

Fig. 7. Liquidus phase relations in the system Qz-Ab-Or-H₂O-CO₂ at 5 kbar for a fluid phase with a $X^{in}_{H_2O} = 0.7$. Experimental results are given in Table 8. Symbols and sources of data as in Figure 2.
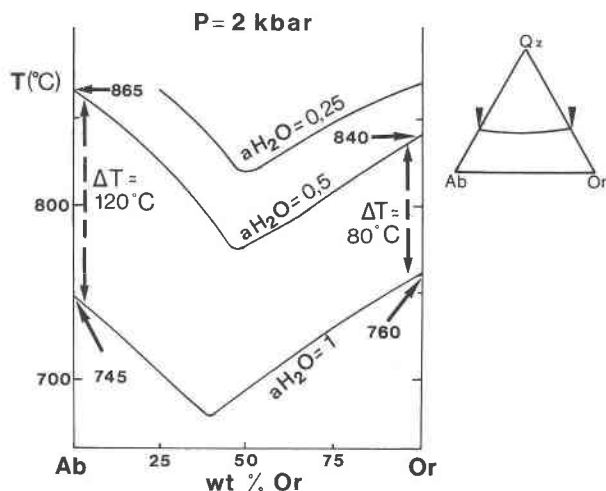
Fig. 8. Section through the liquidus surfaces along the cotectic in the system Qz-Or-Ab-H₂O-CO₂. Note the temperature increase of the liquidus temperature with decreasing a_{H_2O} from 1 to 0.5, which is more important on the Qz-Ab than on the Qz-Or join.

TABLE 12. Compositions and temperatures of minimum liquidus and eutectic points

Ref.	P (kbar)	$X_{H_2O}^{In}$	Qz (wt%)	Or (wt%)	Ab (wt%)	T (°C)
HPBJ*	2	1	36	25	39	685
TB**	2	1	35	26	39	685
HPBJ*	2	0.7	35	29	36	775
HPBJ*	2	0.5	35	31	34	830
HPBJ*	5	1	31	22	47	645
LJT†	5	1	27	23	50	640
HPBJ*	5	0.85	32	25	43	735
HPBJ*	5	0.7	32	28	40	790

* This work.
** Tuttle and Bowen (1958).
† Luth et al. (1964).

tions (see Table 2 for typical standard deviations) that could be attributed to a heterogeneous distribution of H₂O. For the fluid phase, its homogeneous spatial distribution, phase assemblage, volumetric proportion, and volumetric properties (homogenization temperatures within 0.2 °C) in a given sample conclusively suggest homogeneity. In spite of uncertainties in our a_{H_2O} calculations, the identical a_{H_2O} computed from both melt and fluid phases in the same experiment (see above) suggests equilibrium partitioning of the fluid components (H₂O and CO₂) between these two phases.

2. The use of dry starting glasses was adopted to minimize nucleation problems. Fenn (1977) demonstrated that nucleation of alkali feldspar is favored in H₂O-undersaturated melts and at high degrees of undercooling. Both conditions are satisfied during the heating period in our experiments (Pichavant, 1990): H₂O-undersaturated conditions prevail because of the use of initially anhydrous glasses; high degrees of undercooling are also attained, since anhydrous glasses have high liquidus temperatures. In addition, the direct approach to experimental conditions was chosen in both crystallization and reversal experiments. Preconditioning the sample at supraliquidus temperatures causes nucleation problems for feldspars, particularly at low temperatures and H₂O-rich conditions (Naney and Swanson, 1980). Finally, long experimental durations (up to more than 50 d in some reversal experiments) were systematically adopted to avoid incomplete nucleation and growth, especially in experiments below 700 °C. The available data show that the nucleation of silicate phases requires durations ranging from several hours to a few days (Swanson and Fenn, 1986). Comparisons of temperatures indicated by the ends of tie lines and three-phase triangles with the actual temperatures of the experiments do not reveal large differences (maximum 15 °C). This is a strong indication that supercooling problems are minor, since the proportion of crystals in the subliquidus charges is close to the equilibrium proportion. Most feldspars in crystallization experiments have euhedral tabular shapes, indicating a good approach toward equilibrium texture for crystallization at small degrees of undercooling. Some were found to be hollow, however, and they may possibly represent alkali feldspars that nucleated and grew at higher degrees of undercooling, i.e., during the initial stages of the experiment. However, these feldspars must have become chemically indistinguishable from feldspars grown isothermally from a homogeneous hydrous melt because our experimental durations were long enough for attainment of the equilibrium Na-K distribution between alkali feldspar and melt (Johannes, 1985; Pichavant, 1987).

3. In the absence of direct experimental information on the rates of dissolution of quartz and feldspars in haplogranitic melts in the range of 700–900 °C, it is difficult to evaluate precisely the time required for dissolution of crystals in our reversal experiments. Most authors agree, however, that dissolution of crystals in melts is kinetically controlled by diffusion of the components of the crystals in the liquid (Watson, 1982; Donaldson, 1985; Kuo and Kirkpatrick, 1985). Watson (1982) suggested that dissolution of alkali feldspars in basaltic melts at 1200 °C is limited by the diffusivity of SiO₂ and possibly Al₂O₃. If that is the case, that would imply a similar rate of dissolution for quartz and feldspars in our experiments. Given the small and homogeneous sizes of both quartz and alkali feldspars produced in our experiments, superheating problems are not expected during the reversals. Finally, we consider dissolution rates to be at least as fast as growth rates (e.g., Kuo and Kirkpatrick, 1985). Yet, care was taken to keep the durations of the two stages of the reversals approximately identical (Tables 3, 4, 6, 7).

The most conclusive evidence for a close approach to equilibrium is the identity of products and phase compositions in crystallization and reversal experiments. Liquidus temperatures determined from both types of experiments are in agreement (e.g., glass nos. 343, 3₅33₅,
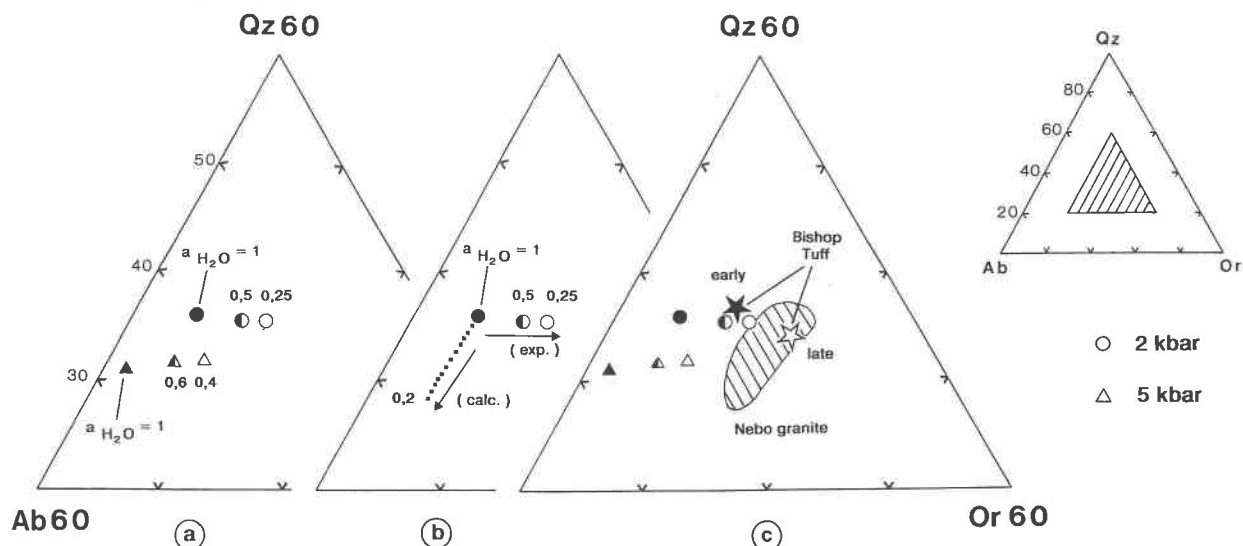
Fig. 9. CIPW normative composition of minimum points, eutectic points, and rocks projected in the Qz-Or-Ab diagram. (a) Diagram showing the progressive shift of the minimum and eutectic point in the Qz-Ab-Or system with decreasing a_{H_2O}, from 1 (filled circle) to 0.50 (half-filled circle) to 0.25 (open circle) at 2 kbar and from 1 (filled triangle) to 0.60 (half-filled triangle) to 0.40 (open triangle) at 5 kbar. (b) Comparison between the experimental shift (this study; circles) and calculated shift (Nek- vasil, 1988; dotted line) of the 2-kbar minimum composition with decreasing a_{H_2O}. (c) Comparison of the CIPW normative compositions of selected subaluminous granitic rocks (filled and open stars representing the early and late Bishop Tuff, respectively; lined area representing the Bushveld Nebo granite) with our experimental results at 2 and 5 kbar and under various a_{H_2O}. See text for further discussion and data sources.

325, Table 4; glass no. 343, Table 6; glass nos. $3_43_33_3$, 334, 2_534_5, Table 7, among others; see the section on liquidus temperatures, above). For a given melt composition, feldspars crystallized in either crystallization or reversal experiments have Or contents within 2 mol% (Tables 4, 6, 7). The general chemical homogeneity of the alkali feldspars within one sample and the absence of compositional zoning suggest a close approach toward chemical equilibrium between melt and crystals in both types of experiments. The only heterogeneous feldspar compositions were encountered for starting compositions with Ab/Or ratios close to 1 and liquidus temperatures above the alkali feldspar solvus (see above and the tables). These may result from small compositional fluctuations in the melt, inducing comparatively large effects on the alkali feldspar composition because of the flat shape of the solidus surface under these particular conditions.

Comparison with previous studies under H₂O-saturated conditions

Our 2-kbar data are in good agreement with those of Tuttle and Bowen (1958). There is no difference within error between the location of our quartz-feldspar cotectic, the temperature, and composition of the minimum (Table 12), on the one hand, and those given by Tuttle and Bowen (1958) on the other. Some minor discrepancies are apparent, however. For the quartz primary field, the liquidus surface is steeper in Tuttle and Bowen (1958) than in our study. This can be explained by differences in experimental procedures: open capsules were used by Tuttle and Bowen (1958) and change of the melt composition toward higher normative Qz probably occurred in their experiments.

In contrast, our results at 5 kbar under H₂O-saturated conditions differ from those of Luth et al. (1964), especially in the position of the quartz-feldspar field boundary. The boundary is richer by 2 wt% normative quartz (on the Qz-Ab side) to 6 wt% normative quartz (on the Qz-Or side) in our study than in Luth et al. (1964). Some compositions that are in the Qz field according to Luth et al. (1964) lie in the Or field in this study (nos. $3_43_72_9$, 3_542_5, Table 6). The new eutectic composition is $Qz_{31}Or_{22}Ab_{47}$ (Table 12) and is richer by 4 wt% normative Qz than that given by Luth et al. (1964). It is worth noting that the largest disagreement between the two data sets is observed for compositions near the Qz-Or binary system, which may be a consequence of the Na contamination that affected the starting gels used by Luth et al. (1964), as discussed by Luth (1976). Because of the displacement of the three liquidus fields in the two studies, isotherms are not directly comparable, especially if we consider the suggestion of Luth (1976) to reduce by 10–15 °C the liquidus temperatures of Luth et al. (1964).

Isobaric effect of H₂O on liquidus phase relationships

The isobaric effect of H₂O on liquidus phase relationships can be evaluated by comparing the phase diagrams obtained with decreasing $X_{H_2O}^{In}$ (a_{H_2O}) and the H₂O content

of the melt. The change in phase relations is similar at 2 and 5 kbar.

Reduction of the H_2O content of the melt causes a rise in the liquidus temperatures for all compositions studied. However, this effect is more pronounced for compositions near the Qz-Ab than the Qz-Or binary system (Fig. 8). Although this behavior was observed at both pressures, the 2-kbar data allow a precise illustration of it. For composition 3_542_5 (Or rich), when compared with 3_524_5 (Ab rich), the increase in liquidus temperatures relative to H_2O-saturated conditions is 65 and 110 °C, respectively, at $X^{ln}_{H_2O} = 0.7$ (Figs. 2, 3). This behavior is also marked in the binary eutectic compositions (80 °C for Qz-Or, 120 °C for Qz-Ab; Pichavant et al., 1992). The temperature of the minimum liquidus composition also rises by 120 °C under these conditions (Figs. 2, 3; Table 12). This effect diminishes progressively with a reduction in $X^{ln}_{H_2O}$ (a_{H_2O}), and the increase in liquidus temperatures becomes smaller between Or- and Ab-rich compositions ($X^{ln}_{H_2O} = 0.5$ at 120 °C for Qz-Or, at 160 °C for Qz-Ab, and at 175 °C for the minimum liquidus composition; Fig. 8; Table 12). In comparison, the 5-kbar minimum liquidus temperatures are raised by 95 °C ($X^{ln}_{H_2O} = 0.85$) and 150 °C ($X^{ln}_{H_2O} = 0.7$). Taken as a whole, the 2- and 5-kbar ternary liquidus surfaces are lifted and shifted toward the Qz-Or binary system. Concomitantly, they become progressively flatter, as shown by the larger compositional interval between isotherms for the two most H_2O-undersaturated sections (Figs. 4, 7) and by the progressively less pronounced temperature well around the minimum liquidus compositions. It is worth recalling that the dry Qz-Or-Ab system at 1 atm has a very flat liquidus surface and that the temperature decrease toward the minimum along the cotectic is small (Schairer and Bowen, 1935; Schairer, 1950).

Since the increase in liquidus temperatures with decreasing $X^{ln}_{H_2O}$ is similar for compositions in the quartz and the alkali feldspar primary fields, the position of the cotectic line for a given pressure is not significantly displaced in terms of its normative quartz content (see Pichavant et al., 1992, for illustration in the Qz-Ab and Qz-Or binary systems at 2 kbar). The minimum liquidus compositions are displaced monotonically with decreasing $X^{ln}_{H_2O}$, the direction of displacement being similar at 2 and 5 kbar. The magnitude of the observed shifts is not directly comparable at the two pressures studied, because the four H_2O-undersaturated isobaric sections are determined for four different a_{H_2O} (Table 11).

Compared with the compositional trend followed by minima and eutectic points with decreasing PH_2O (Tuttle and Bowen, 1958; Luth et al., 1964; Luth, 1976), the displacements with an isobaric decrease of a_{H_2O} are almost orthogonal. Note that two parameters (P and the H_2O content of melt) are varied simultaneously in the former experiments (Tuttle and Bowen, 1958; Luth et al., 1964; Luth, 1976). Pressure is known to have an important intrinsic effect on phase relations under dry conditions (Luth, 1969; Boettcher et al., 1984). On the other hand, our data show the effect of changes in the H_2O content of the melt only. The compositional variations of the minimum liquidus temperature points found in this study are of the same type demonstrated by Pichavant and Ramboz (1985) and Pichavant (1987) in the Qz-Or-Ab-B_2O_3 system at 1 kbar (i.e., a shift toward the Qz-Or join at approximately constant normative Qz content with decreasing a_{H_2O}). Changes in phase relations with a_{H_2O} of the same type as demonstrated in this study and in Pichavant (1987) were also deduced geometrically by Steiner et al. (1975). The phase diagram for a synthetic granite composition at 8 kbar (Whitney, 1975) suggested a displacement of the ternary eutectic toward the Qz-Or join when reducing the H_2O content of the melt. Huang and Wyllie (1975) estimated the 5-kbar dry phase relations in the Qz-Or-Ab system, implying a change in phase relations of the same type as demonstrated here.

Implications for aluminosilicate-H₂O solution models

Nekvasil and Burnham (1987) calculated, using the revised quasi-crystalline model of hydrous silicate melts (Burnham and Nekvasil, 1986), both the liquidus phase relations in the system Qz-Or-Ab at various pressures and the H_2O contents of the melt. Generally good agreement between calculated and experimentally determined liquidus phase relations was obtained for H_2O-saturated isobaric sections. However, the calculations predict a displacement of the 2-kbar minimum liquidus composition toward the Ab-Or join at approximately constant normative Or (Nekvasil, 1988; see also Fig. 9) with progressive reduction in a_{H_2O} and in the H_2O content of the melt. In particular, the normative Qz content of the calculated minimum points vary strongly with a changing H_2O content of the melt, in marked contrast to our experimental results. As an attempt to solve this major discrepancy between calculations (Nekvasil and Burnham, 1987) and our experiments (Holtz et al., 1988; Pichavant et al., 1992; and this paper), Nekvasil and Holloway (1989) conducted a few select experiments. Their data at 5 kbar for a composition of $Qz_{30.5}Or_{10.9}Ab_{58.6}$ and $a_{H_2O} = 1$ are in excellent agreement with our phase diagram in terms of liquidus temperatures, liquidus phases, and the position of field boundaries. They confirm the necessity, demonstrated here, to place the quartz-feldspar field boundary at higher normative Qz contents than that drawn by Luth et al. (1964). However the expansion of the quartz liquidus primary field with decreasing a_{H_2O}, predicted by Nekvasil and Burnham (1987), is not clearly demonstrated in the study of Nekvasil and Holloway (1989).

The discrepancy between experimentally determined phase relations (this work) and calculated phase relations (Nekvasil and Burnham, 1987) may be sought first in our experimental procedures. Our experimental melt compositions straddle the boundary between peralkaline and peraluminous compositions, but most are weakly peraluminous (Table 9). The presence of normative corundum is known to have a small effect on phase relations in the system Qz-Or-Ab (displacement of the cotectic toward the Qz apex by approximately 3 wt% normative Qz in melts saturated with respect to mullite; Holtz et al.,

1992b). However, there is no systematic variation in the normative corundum of our experimental glasses with a_{H_2O} (Table 9). This rules out any influence of the presence of normative corundum on phase relations. Alternatively, all our H_2O-undersaturated experiments were carried out in the presence of CO_2 (whereas calculations assume that no CO_2 is present). Our data show that the solubility of CO_2 in our melt compositions is lower than 0.3 wt%. At these low concentrations, we consider the effect of CO_2 on phase relations to be negligible.

A second possibility is that some assumptions made in the calculations need to be critically reexamined. The aluminosilicate-H_2O solution model of Burnham (1979), used in the calculations of Burnham and Nekvasil (1986) and Nekvasil and Burnham (1987), assumed equimolal isothermal isobaric H_2O solubilities in feldspar melts. In contrast, McMillan and Holloway (1987), Holtz et al. (1992a), and Pichavant et al. (1992) have, among others, drawn attention to the compositional dependence of H_2O solubility in haplogranitic melts (see also Voigt et al., 1981). For example, Holtz et al. (1992a) demonstrated that H_2O solubility depended on composition (Ab/Or ratio) at 2 kbar and 800 °C. For cotectic compositions, H_2O solubilities are higher on the Ab-rich side than on the Or-rich side by 15% (relative) (Holtz et al., 1992a). We conclude that all the recent H_2O solubility data obtained for quartz-feldspar melts disprove the validity of the assumption made by Burnham (1979) concerning equimolal H_2O solubilities in feldspar melts.

The compositional dependence of H_2O solubility in haplogranitic melts shown by Holtz et al. (1992a) implies that H_2O contents vary with melt composition in the ternary phase diagram (see also Tuttle and Bowen, 1958, p. 54). Therefore, our calculated a_{H_2O} only apply to the compositions for which the melt H_2O content was determined, i.e., for compositions close to the minimum. This is an important conclusion that must be taken into account when using such phase diagrams for petrologic interpretations (see below). In addition, the H_2O solubility data provide a simple rationale for the changes in phase relations observed in this paper. Pichavant et al. (1992) suggested that, for a given P, T, and a_{H_2O}, higher amounts of molecular H_2O are incorporated in Ab than in Or melts. Therefore, Na-rich and K-rich units behave in a different manner in response to changes in a_{H_2O}, thus explaining the contrasting behavior observed between Ab-rich and Or-rich compositions. A specific discussion of the experimental results concerning H_2O solubility mechanisms in aluminosilicate melts can be found in Pichavant et al. (1992).

PETROLOGIC APPLICATIONS

Both the H_2O content of the melt and the pressure may vary independently during the evolution of felsic magmas. For example, quasi-isobaric H_2O enrichment in the melt may occur in magma chambers undergoing fractional crystallization of anhydrous phases. Alternatively, magmas may ascend with a constant H_2O content of the melt phase. The present experimental study gives insight to the effect of increasing the H_2O content of the melt on residual melt compositions. This study, coupled with the studies of Luth (1969) and Boettcher et al. (1984) on the effect of pressure, makes it possible to distinguish between the individual effects of P and H_2O content of the melt and to evaluate how the liquid line of descent is affected by simultaneous variations of the two parameters. Before applying the experimental data to natural systems, it should be noted that this discussion applies only to granitic melt compositions in equilibrium with crystallizing quartz and alkali feldspar (or alkali feldspar and plagioclase) among other phases, a situation not necessarily encountered in the crystallization history of all granitic rocks.

Although the principal conclusions of this paper regarding the effect of the H_2O content of the melt on liquidus phase relations are of interest for all types of granites, the experimental results must be applied with caution. A serious problem (apart from obvious troubles arising from late magmatic or deuteric alteration processes) is that granites may well not be representative of their parent melt compositions. Some may contain a significant amount of restite and others may have experienced mechanical fractionation between crystals and liquid, leading to rocks with chemical signatures of cumulates. This is a serious difficulty in the application of liquidus diagrams to the interpretation of granite petrogenesis. Note that the problem is not totally eliminated for all volcanic rocks (ignimbrites or ash-flow tuffs) because of the possibility of mechanical separation between the vitric fraction and phenocrysts during eruption or in the magma chamber.

Two examples have been selected for detailed discussion: (1) the Bishop Tuff from California (Hildreth, 1979) and (2) the Bushveld Nebo granite (Kleeman and Twist, 1989). On the basis of a detailed petrographical and geochemical study, Hildreth (1979) demonstrated a change in the major- and trace-element composition between early, H_2O-rich Bishop Tuff volcanic units (up to more than 6 wt% H_2O, Hildreth, 1979; Anderson et al., 1989) and late, less H_2O-rich ones (3 wt% H_2O, Hildreth, 1979; Anderson et al., 1989; see also Dunbar and Hervig, 1990). This compositional stratification of the magma chamber was attributed by Hildreth (1979) to a convection-driven thermogravitational fractionation process. When plotted on a Qz-Or-Ab diagram (Fig. 9), the representative compositions of the early and late units (bulk rock analyses) define a trend of decreasing normative Or at an approximately constant Qz-Ab ratio. As noted by Hildreth (1979, p. 55), this trend is unrelated to modal phenocryst content, and it diverges from the trend of H_2O-saturated minima and eutectics (e.g., Tuttle and Bowen, 1958; Luth et al., 1964). However, it is similar to the trend experimentally determined in this study for progressively H_2O-rich residual liquid compositions. The somewhat oblique direction of the natural rock trend compared with our isobaric data may reflect a pressure decrease from the early to the late unit (Anderson et al., 1989). Thus, the compositional variation between the early and late Bish-

op Tuff units can be simply attributed to nearly isobaric crystal fractionation of quartz and feldspar phases in a magma that becomes progressively enriched in H_2O. This conclusion is consistent with the estimations of T and H_2O contents of the melt for the two units (Hildreth, 1979). Note that the pressure of around 2 kbar or slightly higher, suggested on the basis of our experimental data for the depth of the Bishop Tuff magma chamber, is in excellent agreement with other estimates (e.g., Anderson et al., 1989).

In contrast, the Bushveld Nebo granite, considered as a typical A-type hypersolvus granite (Kleeman and Twist, 1989) defines a trend almost perpendicular to that of the Bishop Tuff (Fig. 9). It is characterized by an evolution at approximately constant normative Or, with the most chemically fractionated granite types being the richest in normative Qz. All samples are richer in normative Or than the H_2O-saturated minimum compositions, suggesting relatively dry magmatic conditions. Indeed, the H_2O content of the melt was estimated to be around 2.2 wt% by Kleeman and Twist (1989). The major-element composition of the Nebo granite is consistent with a protracted evolution of residual liquids at decreasing pressure. From the plot in Figure 9 (orthogonal to the isobaric effect of a_{H_2O}) the Nebo granite magma seems to have evolved with roughly constant H_2O in the melt.

It is worth noting that the evolution discussed here for the Nebo granite is close to that shown by the 156 alumina-undersaturated plutonic rocks selected by Luth et al. (1964) from Washington (1917). These have normative compositions systematically shifted toward the Qz-Or sideline, when compared to H_2O-saturated minima and eutectics (see Fig. 7 in Luth et al., 1964). Some of these rocks have chemical compositions corresponding to hypersolvus or A-type granites, and it is therefore likely that their normative compositions reflect H_2O-undersaturated rather than H_2O-saturated residual granitic melt compositions.

ACKNOWLEDGMENTS

REFERENCES CITED

Anderson, A.T., Jr., Newman, S., Williams, S.N., Druitt, T.H., Skirius, C., and Stolper, E. (1989) H_2O, CO_2, Cl, and gas in plinian and ash-flow Bishop rhyolite. Geology, 19, 1–42.

Boettcher, A.L. (1984) The system SiO_2-H_2O-CO_2: Melting, solubility mechanisms of carbon, and liquid structure to high pressures. American Mineralogist, 69, 823–833.

Boettcher, A.L., and Wyllie, P.J. (1969) Phase relationships in the system $NaAlSiO_4$-SiO_2-H_2O to 35 kilobars pressure. American Journal of Science, 267, 875–909.

Boettcher, A.L., Guo, Q., Bohlen, S., and Hanson, B. (1984) Melting in feldspar-bearing systems to high pressures and the structure of aluminosilicate liquids. Geology, 12, 202–204.

Boettcher, A., Luth, R.W., and White, B.S. (1987) Carbon in silicate liquids: The systems $NaAlSi_3O_8$-CO_2, $CaAl_2Si_2O_8$-CO_2, and $KAlSi_3O_8$-CO_2. Contributions to Mineralogy and Petrology, 97, 297–304.

Brown, W.L., and Parsons, I. (1980) Towards a more practical two-feldspar geothermometer. Contributions to Mineralogy and Petrology, 76, 369–377.

Burnham, C.W. (1967) Hydrothermal fluids at the magmatic stage. In H.L. Barnes, Ed., Geochemistry of hydrothermal ore deposits (1st edition), p. 34–76. Holt, Reinhard and Winston, New York.

——— (1979) The importance of volatile constituents. In H.S. Yoder, Ed., The evolution of the igneous rocks: Fiftieth anniversary perspectives, p. 439–482. Princeton University Press, Princeton, New Jersey.

——— (1981) The nature of multicomponent aluminosilicate melts. In D.T. Rickard and F.E. Wickman, Eds., Chemistry and geochemistry of solutions at high temperatures and pressures, physics and chemistry of the Earth, p. 13–14, 197–229. Pergamon, New York.

Burnham, C.W., and Nekvasil, H. (1986) Equilibrium properties of granite pegmatite magmas. American Mineralogist, 71, 239–263.

Clemens, J.D. (1984) Water contents of silicic to intermediate magmas. Lithos, 17, 273–287.

Donaldson, C.H. (1985) The rates of dissolution of olivine, plagioclase, and quartz in a basalt melt. Mineralogical Magazine, 49, 683–693.

Dunbar, N.W., and Hervig, R.L. (1990) Volatile gradient within the upper portion of the Bishop magma chamber: Evidence from ion microprobe analyses of melt inclusions. Eos, 71, 651.

Ebadi, A., and Johannes, W. (1991) Experimental investigation of composition and beginning of melting in the system $NaAlSi_3O_8$-$KAlSi_3O_8$-SiO_2-H_2O-CO_2. Contributions to Mineralogy and Petrology, 106, 286–295.

Fenn, P.M. (1977) The nucleation and growth of alkali feldspars from hydrous melts. Canadian Mineralogist, 15, 135–161.

Fogel, R.A., and Rutherford, M.J. (1990) The solubility of carbon dioxide in rhyolitic melts: A quantitative FTIR study. American Mineralogist, 75, 1311–1326.

Goranson, R.W. (1938) Silicate-H_2O systems: Phase equilibria in the $NaAlSi_3O_8$-H_2O and $KAlSi_3O_8$-H_2O systems at high pressures and temperatures. American Journal of Science, 35, 71–91.

Hamilton, D.L., and Oxtoby, S. (1986) Solubility of water in albite melt determined by the weight-loss method. Journal of Geology, 94, 626–630.

Hildreth, W. (1979) The Bishop Tuff: Evidence for the origin of compositional zonation in silicic magma chambers. Geological Society of America Special Paper, 180, 43–75.

Holtz, F., Johannes, W., Barbey, P., and Pichavant, M. (1988) Liquidus phase relations in the system Qz-Ab-Or at 2 kbar: The effect of aH_2O. Eos, 69, 513.

Holtz, F., Behrens, H., Dingwell, D.B., and Taylor, R. (1992a) Water solubility in aluminosilicate melts of haplogranitic compositions at 2 kbar. Chemical Geology, 96, 289–302.

Holtz, F., Johannes, W., and Pichavant, M. (1992b) Effect of excess aluminium on phase relations in the system Qz-Ab-Or. Experimental investigation at 2 kbar and reduced H_2O-activity. European Journal of Mineralogy, 4, 137–152.

Huang, W.L., and Wyllie, P.J. (1975) Melting reactions in the system $NaAlSi_3O_8$-$KAlSi_3O_8$-SiO_2 to 35 kilobars, dry and with excess water. Journal of Geology, 83, 737–748.

——— (1986) Phase relationships of gabbrotonalite-granite-water at 15 kbar with applications to differentiation and anatexis. American Mineralogist, 71, 301–316.

James, R.S., and Hamilton, D.L. (1969) Phase relations in the system $NaAlSi_3O_8$-$KAlSi_3O_8$-$CaAl_2Si_2O_8$-SiO_2 at 1 kilobar water pressure. Contributions to Mineralogy and Petrology, 21, 111–141.

Johannes, W. (1979) Ternary feldspars: Kinetics and possible equilibria at 800 °C. Contributions to Mineralogy and Petrology, 68, 221–230.

——— (1980) Metastable melting in the granite system Qz-Ab-Or-An-H₂O. Contributions to Mineralogy and Petrology, 72, 73–80.

——— (1984) Beginning of melting in the granite system Qz-Ab-Or-An-H₂O. Contributions to Mineralogy and Petrology, 84, 264–273.

——— (1985) The significance of experimental studies for the fomation of migmatites. In J.R. Ashworth, Ed., Migmatites, p. 36–85. Blackie, Glasgow, Scotland.

Keppler, H. (1989) The influence of the fluid phase composition on solidus temperatures in the haplogranite system $NaAlSi_3O_8$-$KAlSi_3O_8$-SiO_2-H_2O-CO_2. Contributions to Mineralogy and Petrology, 102, 321–327.

Kerrick, D.M., and Jacobs, G.K. (1981) A modified Redlich-Kwong equation for H_2O, CO_2 and H_2O-CO_2 mixtures at elevated pressures and temperatures. American Journal of Science, 281, 735–767.

Kleeman, G.J., and Twist, D. (1989) The compositionally-zoned sheetlike granite pluton of the Bushveld Complex: Evidence bearing on the nature of A-type magmatism. Journal of Petrology, 30, 1383–1414.

Kohn, S.C., Dupree, R., and Smith, M.E. (1989) A multinuclear magnetic resonance study of the structure of hydrous albite glasses. Geochimica et Cosmochimica Acta, 53, 2925–2935.

Kuo, L.C., and Kirkpatrick, R.J. (1985) Kinetics of crystal dissolution in the system diopside-forsterite-silica. American Journal of Science, 285, 51–90.

Lapham, K.E., Holloway, J.R., and Delaney, J.R. (1984) Diffusion of H_2O and D_2O in obsidian at elevated temperatures and pressures. Journal of Non-Crystalline Solids, 67, 179–191.

Luth, W.C. (1969) The systems $NaAlSi_3O_8$-SiO_2 and $KAlSi_3O_8$-SiO_2 to 20 kb and the relationship between H_2O-content, P_{H_2O}, and P_{total} in granitic magmas. American Journal of Science, A-267, 325–341.

——— (1976) Granitic rocks. In D.K. Bailey and R. MacDonalds, Eds., The evolution of the crystalline rocks, p. 335–417. Academic Press, London.

Luth, W.C., Jahns, R.H., and Tuttle, O.F. (1964) The granite system at pressures of 4 to 10 kilobars. Journal of Geophysical Research, 69, 759–773.

Maaloe, S., and Wyllie, P.J. (1975) Water content of a granitic magma deduced from the sequence of crystallization determined experimentally with water-undersaturated conditions. Contributions to Mineralogy and Petrology, 52, 175–191.

McMillan, P.F., and Holloway, J.R. (1987) Water solubility in aluminosilicate melts. Contributions to Mineralogy and Petrology, 97, 320–332.

Merrill, R.B., Robertson, J.K., and Wyllie, P.J. (1970) Melting reactions in the system $NaAlSi_3O_8$-$KAlSi_3O_8$-SiO_2-H_2O to 20 kilobars compared with pressures for other feldspar-quartz-H_2O and rock-H_2O systems. Journal of Geology, 78, 558–569.

Naney, M.T., and Swanson, S.E. (1980) The effect of Fe and Mg on crystallization in granitic systems. American Mineralogist, 65, 639–653.

Nekvasil, H. (1988) Calculated effect of anorthite component on the crystallization paths of H_2O-undersaturated haplogranitic melts. American Mineralogist, 73, 966–981.

Nekvasil, H., and Burnham, C.W. (1987) The calculated individual effects of pressure and water content on phase equilibria in the granite system. Geochemical Society Special Publication 1, 433–445.

Nekvasil, H., and Holloway, J.R. (1989) H_2O-undersaturated phase relations in the system Qz-Ab-Or-H_2O: New considerations. Eos, 70, 506.

Orville, P.M. (1963) Alkali ion exchange between vapor and feldspar phases. American Journal of Science, 261, 201–237.

Pichavant, M. (1987) Effects of B and H_2O on liquidus phase relations in the haplogranite system at 1 kbar. American Mineralogist, 72, 1056–1070.

——— (1990) Phase equilibria in granitic systems: Implications for H_2O speciation in aluminosilicate melts. Terra Abstracts, 2, 28.

Pichavant, M., and Ramboz, C. (1985) Première détermination expérimentale des relations de phases dans le système haplogranitique en conditions de sous-saturation en H_2O. Comptes Rendus de l'Académie des Sciences de Paris, 301, 607–610.

Pichavant, M., Kontak, D.J., Briqueu, L., Valencia Herrera, J., and Clark, A.H. (1988) The Miocene Pliocene Macusani volcanics, S.E. Peru. I. Mineralogy and magmatic evolution of a two-mica aluminosilicate-bearing ignimbrite suite. Contributions to Mineralogy and Petrology, 100, 300–324.

Pichavant, M., Holtz, F., and McMillan, P. (1992) Phase relations and compositional dependence of H_2O solubility in quartz-feldspar melts. Chemical Geology, 96, 303–319.

Puziewicz, J., and Johannes, W. (1988) Phase equilibria and compositions of Fe-Mg-Al minerals and melts in water-saturated peraluminous granitic systems. Contributions to Mineralogy and Petrology, 100, 156–168.

Ramboz, C., Schnapper, D., and Dubessy, J. (1985) The P-V-T-X-f_{O_2} evolution of H_2O-CO_2-CH_4-bearing fluid in a wolframite vein: Reconstruction from the fluid inclusion studies. Geochimica et Cosmochimica Acta, 49, 205–219.

Schairer, J.F. (1950) The alkali feldspar join in the system $NaAlSi_3O_8$-$KAlSi_3O_8$-SiO_2. Journal of Geology, 58, 512–517.

Schairer, J.F., and Bowen, N.L. (1935) Preliminary report on equilibrium relations between feldspathoids, alkali feldspars, and silica. Transactions of the American Geophysical Union, 16, 325–328.

Shaw, H.R. (1974) Diffusion of H_2O in granitic liquid. I—Experimental data. II—Mass transfer in magma chambers. In A.W. Hofmann, B.J. Giletti, H.S. Yoder, Jr., and R.A. Yund, Eds., Geochemical transport and kinetics, publication 634, p. 139–170. Carnegie Institution of Washington, Washington, DC.

Silver, L., and Stolper, E.M. (1989) Water in albitic glasses. Journal of Petrology, 30, 667–710.

Silver, L.A., Ihinger, P.D., and Stolper, E. (1990) The influence of bulk composition on the speciation of water in silicate glasses. Contributions to Mineralogy and Petrology, 104, 142–162.

Steiner, J.C., Jahns, R.H., and Luth, W.C. (1975) Crystallization of alkali feldspar and quartz in the haplogranite system $NaAlSi_3O_8$-$KAlSi_3O_8$-SiO_2-H_2O at 4 kb. Geological Society of America Bulletin, 86, 83–98.

Stolper, E.M. (1982) Water in silicate glasses: An infrared spectroscopic study. Contributions to Mineralogy and Petrology, 81, 1–17.

Swanson, S.E., and Fenn, P.M. (1986) Quartz crystallization in igneous rocks. American Mineralogist, 71, 331–342.

Tuttle, O.F., and Bowen, N.L. (1958) Origin of granite in the light of experimental studies in the system $NaAlSi_3O_8$-$KAlSi_3O_8$-SiO_2-H_2O. Geological Society of America Memoir 74, 145 p.

Voigt, D.E., Bodnar, R.J., and Blencoe, J.G. (1981) Water solubility in melts of alkali feldspar composition at 5 kbar, 950 °C. Eos, 62, 428.

Washington, H.S. (1917) Chemical analyses of igneous rocks. U.S. Geological Survey Professional Paper 99, 1201 p.

Watson, E.B. (1982) Basalt contamination by continental crust: Some experiments and models. Contributions to Mineralogy and Petrology, 80, 73–87.

Westrich, H.R. (1987) Determination of water in volcanic glasses by Karl-Fischer titration. Chemical Geology, 63, 335–340.

Whitney, J.A. (1975) The effects of pressure, temperature and X(H_2O) on phase assemblage in four synthetic rock compositions. Journal of Geology, 83, 1–31.

Winkler, H.G.F. (1979) Petrogenesis of metamorphic rocks (5th edition). Springer, Berlin.

Wyllie, P.J., and Tuttle, O.F. (1959) Effect of carbon dioxide on the melting of granite and feldspars. American Journal of Science, 257, 648–655.

——— (1960) Experimental investigation of silicate systems containing two volatile components: I—Geometrical considerations. American Journal of Science, 258, 497–517.

——— (1961) Experimental investigation of silicate systems containing two volatile components: II—The effects of NH₃ and HF, in addition to H₂O, on the melting temperatures of albite and granite. American Journal of Science, 259, 128–143.